FEASIBILITY OF USING PETROLEUM SEISMIC METHODS TO RESOLVE THIN BEDS IN SALT

by

Scott L. Stockton

ProQuest LLC.
789 East Eisenhower Parkway
P.O. Box 1346
Ann Arbor, MI 48106 – 1346

A Thesis submitted to the Faculty and the Board of Trustees of the Colorado School of Mines in partial fulfillment of the requirements for the degree of Master of Science - Geophysical Engineering.

Signed: Scott L. Stockton
Scott L. Stockton

Golden, Colorado

Date: 3 Sept, 1976

Approved: Frank A. Hadsell
Frank A. Hadsell
Thesis Advisor

George V. Keller
George V. Keller
Head of Department

Golden, Colorado

Date: 9-3, 1976

ABSTRACT

The Energy Research and Development Administration is currently investigating the possibility of using the Salt Valley anticline in the Paradox basin of southeastern Utah for the retrievable storage of solid nuclear waste. Delineation of thin, fluid-saturated interbeds within the salt core of this structure will allow isolation of the waste from the environment.

Analysis of 50 kilometers of conventional reflection seismic data using surface arrays and both impulsive (dynamite) and controlled (Vibroseis*) sources indicates that the potential exists for shallow mapping of high acoustic impedance thin beds in an essentially homogeneous salt. However, computer ray-trace modeling of hypothetical thin beds in salt reveals that the frequency and spatial resolution of most available petroleum seismic data is insufficient to provide the required detail needed for mapping very thin (5 - 70 meters) grossly deformed interbeds at shallow depths (less than 750 meters). For these data, frequencies on the order 500 - 1000 hertz and surface array lengths of less than 350 meters are recommended. Further consideration should be given to the burial of sources and receivers in order to attenuate surface noise.

Correlation of the reflection seismic data with available well data and surface geology over linear salt-cored anticlines in the northwest

*Trademark Continental Oil Company

Paradox basin, Utah reveals a complex, structurally initiated piercement diapir whose upward flow was maintained by rapid contemporaneous flank deposition of continental clastics. Severe collapse faulting near the crests of these structures has distorted the seismic response. Evidence exists, however, that intra-salt thin beds of anhydrite, dolomite and black shale are mappable either as short, discontinuous segments or as amplitude anomalies within the salt due to buried focusing. Computer modeling of the folded interbeds confirms both of these as possible causes for the intra-salt seismic response observed on the data.

Prediction of the seismic signatures from the interbeds can be made from computer simulation of the subsurface acoustic paramaters and geometry. For impulsive source data, a minimum phase wavelet provides a good approximation to the thin bed signature. However, as interbed thicknesses approach the wavelength of the assumed wavelet, interference between reflections from the top and bottom of the thin beds distort the signature and a symmetrical signature results.

The major difficulty in using petroleum seismic reflection data to map thin, high-impedance interbeds in salt is the lack of sufficient fidelity to provide direct evidence of their presence. However, the indirect indications present on these data as discontinuous seismic events suggests that refinements and different geophysical techniques would allow direct detection of the interbeds in salt. These methods should include:

a.) Vertical seismic profiling.

b.) Shallow, short-offset, high-frequency seismic reflection

recording.

c.) Detailed borehole survey.

Results of this study may provide guidelines for the approach to other geophysical problems requiring detailed shallow mapping of thin high impedance layers in an essentially homogeneous medium.

TABLE OF CONTENTS

ILLUSTRATIONS

LIST OF SYMBOLS

Symbol	Definition
AGC	Automatic gain control
ΔT	Difference in seismic two-way travel times
T_o	Two-way travel time with seismic source and detector at the same surface location
X	Offset between seismic source and detector
V, V_{nmo}	Stacking velocity
V_{rms}	Root-mean-square velocity
α	Angle of apparent dip
ω	Discrete frequency variable
k	Discrete wave number variable
$\Psi(\omega,k)$	Two-dimensional Fourier Transform
f(t,x)	Two-dimensional time-space function (seismic section)
exp	Exponent
j	Square-root of negative 1
t	Discrete time variable
x	Discrete space variable
db	Decibels
R_{12}	Reflection coefficient between layers 1 and 2
ρ	Density
V_1, V_2	Interval velocity in layer 1 and in layer 2 respectively
cm	Centimeters
θ_1, θ_2	Angles of incidence or refraction in layers 1 or 2

Symbol	Definition
F_n	Nyquist frequency
Δt	Sampling interval
ms	Milliseconds
m	Meters
CDP	Common-depth-point
Hz	Hertz
sec	Seconds

GEOLOGIC SYMBOLS

Symbol	Definition
IPm	Molas Formation (Pennsylvanian)
IPp	Paradox Member, Hermosa Formation (Pennsylvanian)
IPh	Hermosa Formation (Pennsylvanian)
Pc	Cutler Formation (Permian)
TRm	Moenkopi Formation (Triassic)
TRc	Chinle Formation (Triassic)
TRgc	Glen Canyon Group (Triassic)
Jsr	San Rafael Group (Jurassic)
Je	Entrada Formation (Jurassic)
Jm	Morrison Formation (Jurassic)
Kd	Dakota Formation (Cretaceous)
Km	Mancos Formation (Cretaceous)

ACKNOWLEDGMENTS

It is a distinct pleasure to express my appreciation to those organizations and individuals who made this study possible.

I am indebted to Dr. Robert Ryder of the Branch of Oil and Gas Resources, United States Geological Survey, who provided invaluable advice and assistance in establishing the geologic framework for this study. I also thank Dr. Al Balch for suggesting the topic. Grateful appreciation is extended to Messrs. Leonard M. Gard and Robert J. Hite of the U.S.G.S. for their helpful suggestions.

I wish to thank the members of my thesis committee: Dr. Tom Davis, Dr. Phil Romig, Dr. Maurice Major, and especially my advisor, Dr. Frank Hadsell, for their continued support and guidance during the course of this study.

Special thanks to Continental Oil Company for permission to publish their seismic profile (Line C) in this report. I would like to thank the Branch of Oil and Gas Resources for the use of their computing facility at the Denver Federal Center and Seismograph Service Corporation for supplying the modeling system software.

Financial support from the Branch of Special Projects, U.S.G.S., and the Colorado School of Mines made this study possible.

Finally, I would like to thank my wife, Nancy, for her constant encouragement and for her help with the drafting of the illustrations and proofreading of the manuscript.

INTRODUCTION

The Salt Valley anticline, a major linear salt diapir in the Paradox Basin of southeastern Utah (Fig. 1), is currently under consideration by the Energy Research and Development Administration (ERDA) as a possible location for the retrievable storage of highly-radioactive, thermally-hot, solid nuclear waste. The Salt Valley anticline qualifies as a potential waste emplacement site because:

a.) It is a geologically stable feature (Hite and Lohman, 1973);

b.) It is located in an area which is geographically remote but accessible by existing modes of transportation;

c.) It has historically been an area of little or no economic interest.

Another important criterion, the degree of isolation of the diapir from the adjacent environment, has yet to be fully evaluated.

Well control in adjacent diapiric structures and the detailed mapping of the Cane Creek anticline (Evans and Linn, 1970), where a commercial potash mine is located reveals the presence of intensely deformed thin (5 - 70 meters) interbeds of anhydrite, dolomite, and black shale[1] within the halite core. These thin beds are known to contain local accumulations of connate water and over-pressured hydrogen sulfide gas (Leonard M. Gard, oral commun., 1976). The major objective of this report is to determine whether or not the distribution of the high impedance thin beds can be

[1]The "black shale" referred to in much of the literature is, in fact, organic-rich dolomite. This convention will be maintained in this report.

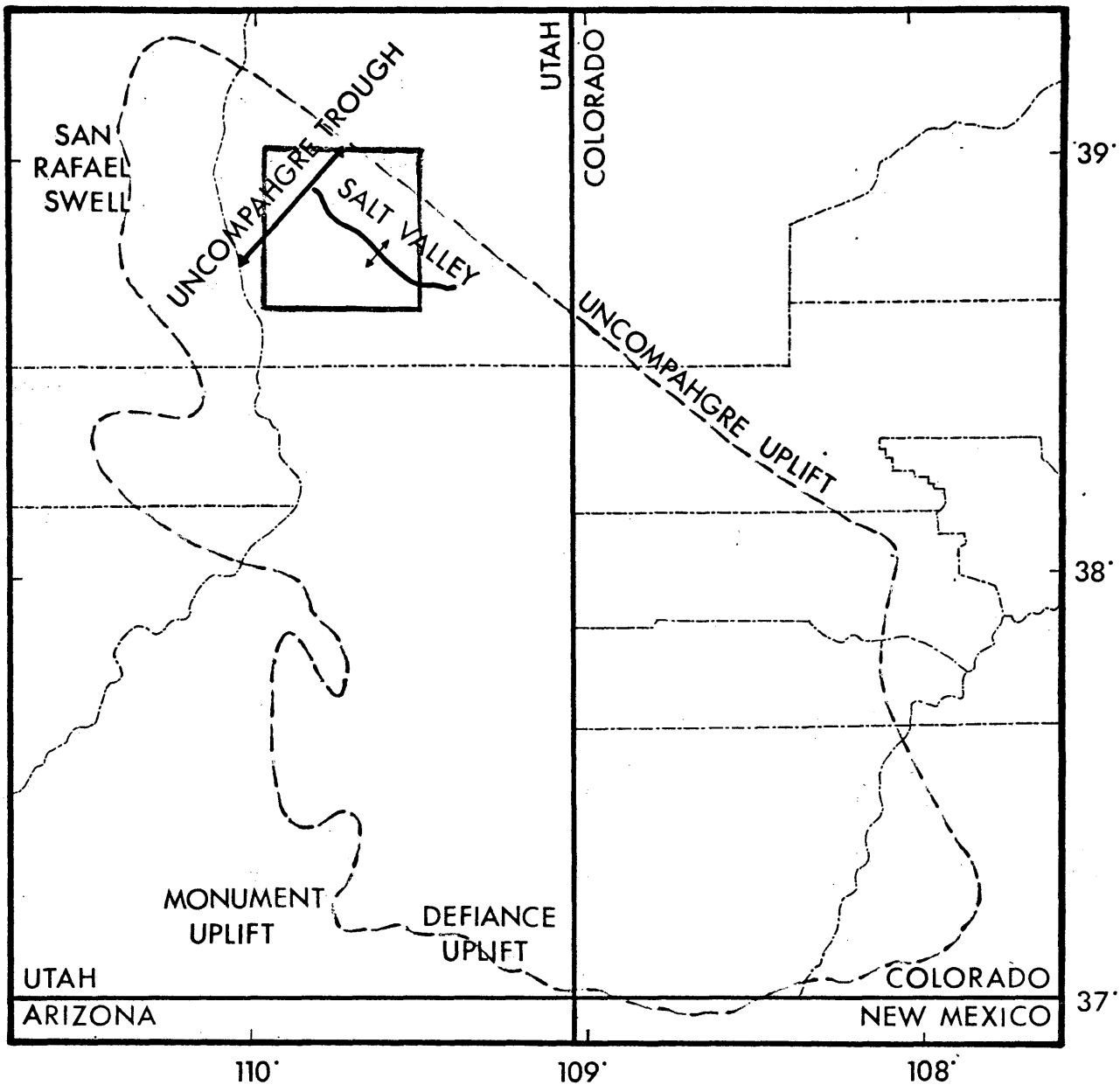

FIGURE 1.
PARADOX BASIN

0 15 30 miles

Approximate limits of Paradox Basin

Study Area

from Hite and Lohman, 1973

detected at shallow depths (less than 750 meters) from conventional petroleum seismic reflection data. Additional objectives include:

a.) The interpretation and correlation of existing seismic data, borehole data and surface geology (Fig. 2) and the analysis of the growth history of the Salt Valley anticline.

b.) The determination of the minimum acceptable seismic resolution needed and the maximum obtainable with conventional methods.

c.) The isolation and identification of seismic signatures from thin beds in a homogeneous medium.

d.) The proposal of recommendation for further studies and the possible applications in other areas of similar subsurface geometry and high acoustic contrast.

Three multi-fold seismic reflection profiles (50 km) obtained from the petroleum industry were extensively processed and interpreted. Moreover, a subsurface, ray-trace, computer modeling system was used to formulate hypothetical models of both the internal and external structure of a salt anticline. The resultant synthetic seismic sections were used to test the validity of the interpretation. The computer modeling was further used to define resolution problems inherent in digital seismic reflection profiling and to suggest possible solutions applicable to the specific problem.

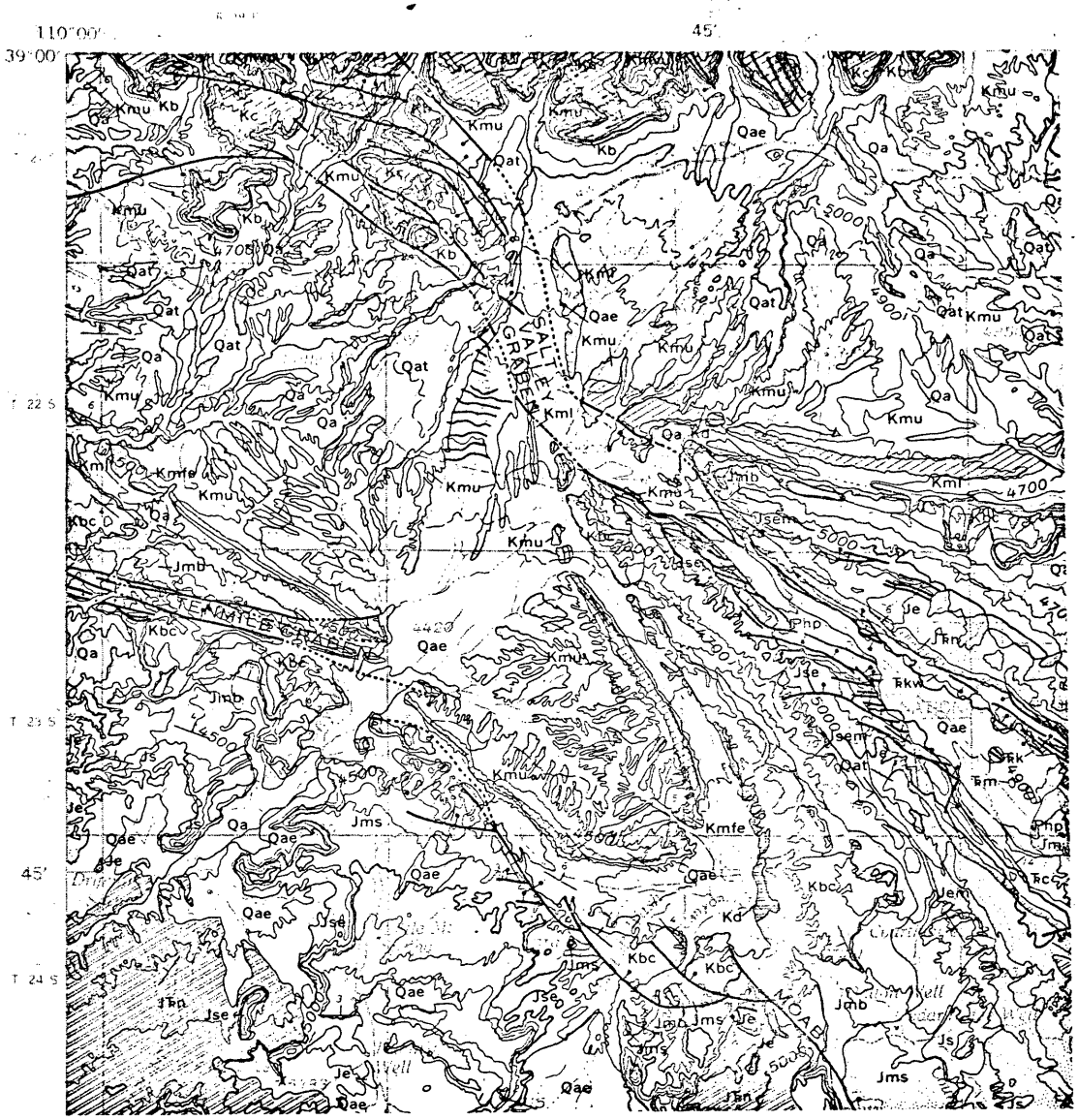

FIGURE 2 - SURFACE GEOLOGY MAP OF THE SALT VALLEY ANTICLINE, PARADOX BASIN, UTAH.

(FROM WILLIAMS, 1964)

REGIONAL GEOLOGIC SETTING

The Paradox basin (Fig. 1) covers approximately 25,000 square kilometers of southern Colorado and Utah. The basin extends roughly northwestward from the Four Corners area. It is flanked by the Monument and Defiance uplifts on the south, the San Rafael swell on the northwest, and the Uncompahgre uplift to the northeast. The eastern edge of the Paradox basin is marked by the San Juan mountain range of south-central Colorado. The southwestern part of the Paradox basin contains the Aneth field where oil is produced from an algal mound of Pennsylvanian age. The Pennsylvanian strata in the basin consist of continental and shallow marine shale and sandstone units which grade basinward into shelf carbonates and evaporites. In the deepest part of the basin (designated the Uncompahgre trough by Hite and Lohman, 1973), the evaporite units have flowed extensively so that they now form a northwest-southeast trending belt of salt-cored anticlinal structures. The Salt Valley anticline lies at the northwest end of this trend. It is an extension of the Fisher Valley and Sinbad Valley anticlines to the southeast. The Salt Valley anticline is bounded by the Courthouse syncline and the Sevenmile anticline to the south. It thins dramatically to the north where sediments are truncated against faulted Precambrian crystalline rocks. Solution by ground water near the surface of these linear diapirs has resulted in the collapse of younger strata into long graben structures. These grabens are manifested in the present topography by flat, linear valleys which are covered with

a thin veneer of Quaternary alluvium. Percolation of ground water and chemical leaching of trace minerals in the shallow sediments has resulted in the formation of a thick, resistant cap over the salt. In the Salt Valley anticline, the cap rock reaches the surface and extends to 200 - 250 meters in depth.

STRATIGRAPHIC FRAMEWORK AND ASSOCIATED ACOUSTIC PROPERTIES

The post-Mississippian lithologies in the Salt Anticline region and their acoustic properties are summarized in Table 1 and in Fig. 3. The remainder of this section discusses these characteristics in detail.

The oldest post-Mississippian strata in the vicinity of the Salt Valley anticline are represented by the Molas Formation (Pennsylvanian). It rests unconformably on Mississippian karst topography and consists of conglomerates, red claystone and siltstone units, and locally, fossiliferous, brown-grey limestone. The Molas is not generally present regionally, but it is identifiable in many of the wells close to the Salt Valley anticline (Hite, 1960).

The Molas Formation is overlain by the Hermosa Group of Pennsylvanian age. In ascending order, the Hermosa is subdivided into the Pinkerton Trail Formation, the Paradox Formation, and the Honaker Trail Formation (Peterson and Ohlen, 1963). Other authors, notably Hite and Lohman (1973), and Cater (1970), classify the Hermosa as a formation and the three divisions as the Lower Member, Paradox Member, and Upper Member respectively. The Lower Member of the Hermosa Formation consists of anhydrite, organic-rich limestone and shale units, and local dolomite and salt. The Lower Member of the Hermosa Formation grades vertically into the overlying Paradox Member. This unit consists principally of salt. The Paradox salt is the principal diapiric rock in the Paradox basin. Original thickness of the salt may have been 1,500 to 2,500 meters (LeFond, 1969), but solution and

SYSTEM	FORMATION			THICKNESS (METERS)	LITHOLOGY	ACOUSTIC PROPERTIES	
						VELOCITY (M/SEC)	DENSITY (GM/CM^3)
CRETACEOUS	Mancos			610±	Dark gray, fissile, marine shale	3,850 - 3,950	2.30 - 2.32
	Dakota			6 - 60	Interbedded sandstone and conglom. carbonaceous shale, impure coal.	3,725 - 3,825	2.36 - 2.41
	Burro Canyon			0 - 90	Sandstone and conglomerate, green and reddish purple shale.		
JURASSIC	Morrison	Brushy Basin Member		90 - 230	Variegated, bentonitic mudstone, siltstone, red ss., conglom., ls. beds.	3,275 - 3,400	2.29 - 2.35
		Salt Wash Member		70 - 135	Lenticular sandstones, few thin limestones.		
	San Rafael Group	Summerville		0 - 30	Thin-bedded sandstone, sandy shale and mudstone.	3,200 - 3,300	2.31 - 2.35
		Entrada	Moab Member	0 - 90	White, cross-bedded, fine-grained sandstone.	3,100 - 4,250	2.35 - 2.49
			Slick Rock Member		Cross-bedded, buff, orange and white, fine-grained sandstone.		
			Dewey Bridge Member	0 - 45	Red, earthy sandstone and siltstone Contorted bedding.		
TRIASSIC	Glen Canyon Group	Navajo		0 - 150	Buff and gray, cross-bedded, fine-grained sandstone.	3,850 - 3,950	2.40 - 2.42
		Kayenta		0 - 90	Lenticular, channel sandstone, siltstone, and mudstone.	3,750 - 3,900	2.39 - 2.43
		Wingate		0 - 150	Fine-grained, reddish-brown, thick-bedded, massive and cross-bedded, cliff-forming sandstone.	3,875 - 4,000	2.44 - 2.46
	Chinle			0 - 230	Reddish siltstone, sandstone, mudstone, and some conglomerate.	4,150 - 4,300	2.45 - 2.55
	Moenkopi			0 - 370	Brown shale, mudstone, arkosic sandstone and conglomerate. Thin beds of gypsum near base.	4,200 - 5,350	2.53 - 2.57
PERMIAN	Cutler			0 - 2,750	Red, arkosic sandstone and conglom. Some red sandy siltstone and mudstone.	4,575 - 4,700	2.46 - 2.55
	Rico			0 - 175	Similar to Cutler, but contains few beds of marine limestone.		
PENNSYLVANIAN	Hermosa		Upper Member	0 - 670	Fossiliferous, gray limestone, shale, and lenticular sandstones.	4,875 - 5,650	2.40 - 2.50
			Paradox Member	0 - 4,280±	Salt, dolomite, gypsum. Carbonaceous shale and sandstone.	4,480±	2.12 - 2.16

TABLE 1. PALEOZOIC AND MESOZOIC STRATIGRAPHY AND ACOUSTIC PROPERTIES NORTHWEST PARADOX BASIN (Stratigraphy after Hite and Lohman, 1973)

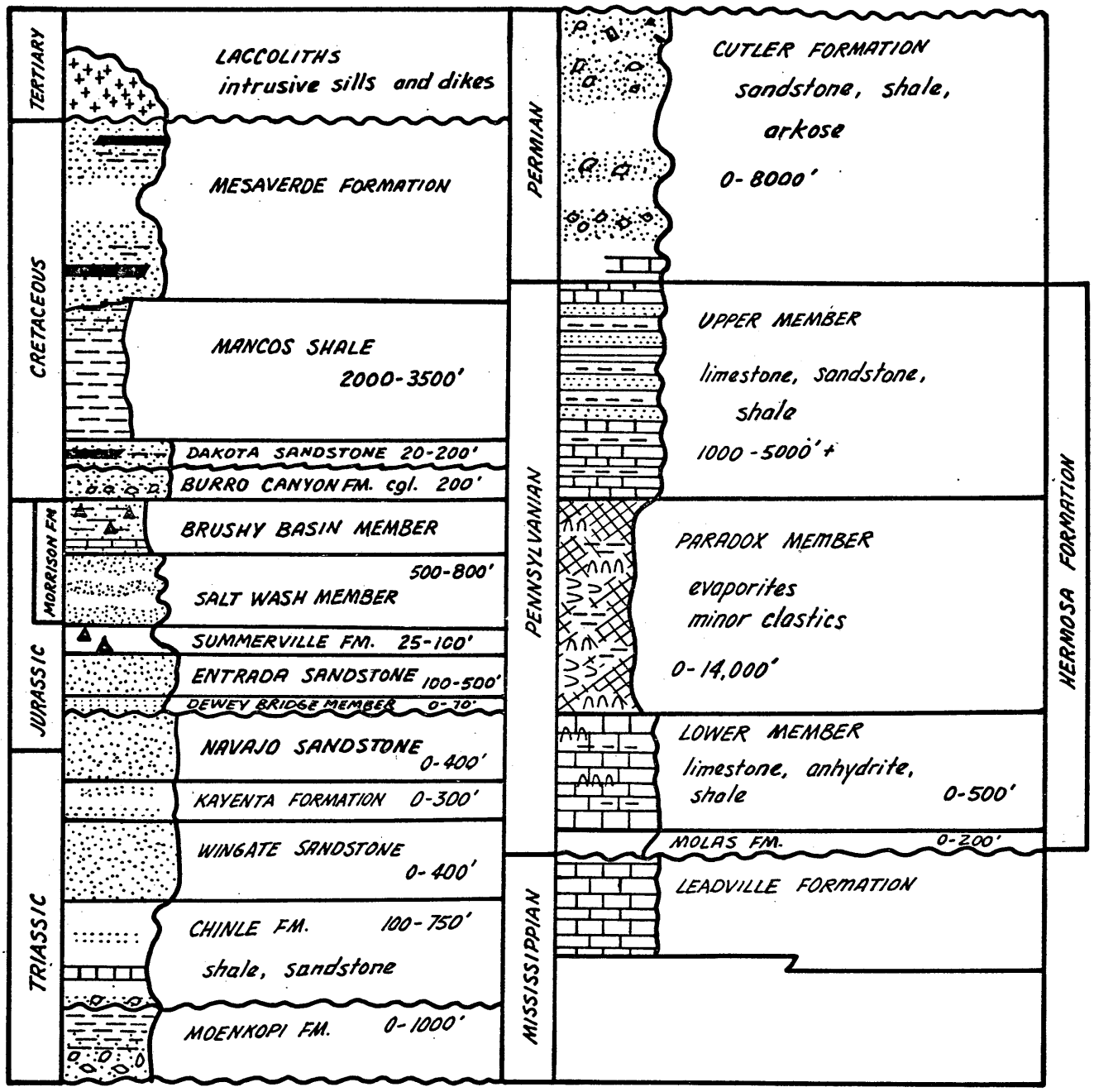

FIGURE 3.
GENERALIZED PALEOZOIC AND MESOZOIC
STRATIGRAPHIC SECTION
OF PARADOX BASIN

adapted from Hite and Lohman, 1973

plastic flow have completely eliminated the salt in some areas while concentrating as much as 4,300 meters of halite in the adjacent anticlinal cores. The base of the Paradox Member is characterized by a high concentration of anhydrite, black shale, and dolomitic limestone interbeds with some potash stringers. The presence of these interbeds is markedly reduced in the upper part of the Paradox Member where thick layers of almost pure halite are evident. In other parts of the Paradox basin, the interbeds within the Paradox salt have been designated as the Ismay, Desert Creek, Akah, and Barker Creek Cycles (Peterson and Ohlen, 1963). Hite (1961) numerically identified nearly thirty distinct cycles of salt, anhydrite, and black shale in the Cane Creek anticline, but correlation between these data and those available in the Salt Valley anticline is poor. The thick Upper Hermosa Member (Honaker Trail Formation) contains fluvial, poorly-sorted, calcareous siltstones, arkosic sandstones, and carbonates. The Upper Hermosa Member is commonly missing over the crests of the anticlines, but is thicker toward the basin axes on the flanks of the structures. The high acoustic contrast between the Upper Hermosa and the low density-velocity Paradox salt results in a sharp negative reflection coefficient which can be expected to map as a trough on a seismogram, while the opposite contrast exists at the boundary between the Paradox Member and the high-velocity, high-density Lower Member (Pinkerton Trail Formation). This interface, then, should appear as a distinct peak on a seismic profile.

The Cutler Formation of Permian age is the thickest sedimentary unit in the Salt Anticline region. It generally lies conformably on the Hermosa Group although detailed geologic mapping indicates that this contact may

be locally unconformable (Cater, 1970). The drastically varying thickness in the Cutler (0 - 2,750 meters) and the variation in lithic characteristics throughout this unit indicate extremely rapid sedimentation and subsidence. The lower part of the Cutler consists of poorly-sorted arkosic sandstone, siltstone, and conglomerate units of fluvial origin, whereas the upper part is arkose and red shale of fluvial origin, and relatively clean quartzose sandstone of aeolian origin. The base of the Cutler Formation contains a resistant marine limestone which, although persistent, is not always identifiable as a separate unit. This is called the Rico Formation is some references (Elston and Landis, 1960).

The Triassic System is represented in ascending order by the Moenkopi Formation, the Chinle Formation, and the Glen Canyon Group. The Moenkopi rests unconformably on the Cutler Formation and consists of shallow-marine brown shale, mudstone and arkosic sandstone units. Thin gypsum beds are found throughout the Moenkopi Formation. The middle Triassic Chinle Formation is primarily fluvial in origin and contains well-sorted clastics interbedded with limestone and dolomite. A pebbly conglomerate unit is located near the base. The Chinle Formation provides a good acoustic contrast, and usually appears as a reflection peak (positive reflection coefficient), and a dependable seismic index marker except in zones where it is intensely fractured. The Glen Canyon Group, consisting in ascending order of the resistant Wingate, Kayenta, and Navajo Formations, forms many of the plateaus cropping out on the flanks of the salt ridges in the Paradox basin. The Wingate is primarily sandstones and siltstones of fluvial origin with minor shelf carbonates and trace

mineralization. The Kayenta Formation consists of alternating pink micaceous sandstone, siltstone, and shallow marine shales. Diagenetic kaolin is present in most of the sandstone cycles within the Kayenta. The upper formation in the Glen Canyon Group, the Navajo Formation, is clean, poorly-cemented sandstone with well-rounded grains. The Navajo Formation is of aeolian origin. The Glen Canyon Group, although a ridge former in the Salt Anticline region, is usually difficult to map seismically because of low acoustic contrast with the overlaying strata, and because the thickness averages less than 200 meters (Hite and Lohman, 1973).

Another unconformity is present between the Navajo and the Entrada Formations. The Entrada Formation, of Jurassic age, is the lower unit in the San Rafael Group which also includes the Summerville Formation. The Entrada is further subdivided into three members which in ascending order are: 1.) the Dewey Bridge Member consisting of redbeds, sandstones, and siltstones; 2.) the Slick Rock Member consisting of clean, fine-grained sandstone; and 3.) the Moab Member which is very clean, white, fine-grained sandstone. The members within the Entrada Formation are not all present regionally, but form tongues which give rise to the wide vertical lithic variations in the Entrada Formation. The Entrada has a marked vertical gradient in its interval velocity and generally, the Entrada-Navajo interface is mappable on a seismic section as a distinct trough. The upper unit in the San Rafael Group, the Summerville Formation, is a thin sequence of sandstone, mudstone, and shallow-marine shale. Because the velocity and density contrast between the Summerville and the Moab Member of the Entrada Formation is slight, this interface is

difficult to map on most seismic profiles.

The Morrison Formation, of Late Jurassic age, conformably overlies the Summerville Formation. The Morrison is divided into two members; the older Salt Wash Member, which consists of sandstones and fresh water limestones, and the younger Brushy Basin Member which contains bentonitic mudstone, red sandstone, limestone, siltstone, and a thin conglomerate. The Morrison Formation provides a good acoustic contrast with the Summerville Formation, and this interface is likely the one being mapped as the top of the Entrada Formation on many seismic sections. Where present, this contact is mappable as a seismic trough.

The Burro Canyon Formation of Cretaceous age lies conformably on the Brushy Basin Member of the Morrison. This formation is not regionally represented in the Paradox basin, but exists in the locality of the Salt Valley anticline. In many areas, there is little or no distinction made between the sandstone, conglomerate, and variegated shale of the Burro Canyon Formation and the lithologies in the overlying Dakota Formation. The principal distinction between the Burro Canyon Formation and the Dakota Formation, which is also of Cretaceous age, is an unconformity which is apparent is some areas. The top of the Dakota Formation provides the best shallow seismic marker in the area. The Dakota consists of coarse, resistant sandstone, variegated shale, local coal seams, and a basal chert-pebble conglomerate.

The youngest stratagraphic unit in the Salt Anticline region is the Mancos Formation (Cretaceous). The Mancos is a friable, fossiliferous,

dark-grey shale of marine origin. Some interbedding of the Mancos with sandstone and bentonite occurs at depth. Except where it is thinly covered with Quaternary alluvium, the thick Mancos shale is a shallow cover in the Salt Valley anticline area and throughout most of the northwestern Paradox basin.

INVESTIGATIVE PROCEDURES

The investigation of the Salt Valley anticline region was divided into four phases:

a.) acquisition of seismic reflection data and analysis of field parameters;

b.) experimental seismic data processing in order to obtain maximum resolution from the existing seismic profiles;

c.) creation of synthetic seismograms from integrated acoustic logs and correlation with the seismic data and other subsurface well log information; and

d.) computer modeling of hypothetical subsurface geology.

The computer subsurface modeling, due to its interpretive nature and broad scope, will be discussed later in this paper.

Seismic Field Parameters

Three multi-fold common-depth-point seismic profiles, one over the Salt Valley anticline, were obtained from the petroleum industry. The principal area of interest for these industry sources was the deeper flank and basal Mississippian sediments rather than interior salt structure. A summary of the seismic field parameters for the three profiles is presented in Table 2. The seismic cross sections for these Lines A, B, and C appear in Fig. 4, 5, and 6 respectively. Line C (Fig. 6) is over the northwestern tip of the Salt Valley anticline where the northwestern plunging trend is interrupted by a small saddle and structural knob

FIELD PARAMETER	LINE A	LINE B	LINE C
SOURCE	Dynamite	Dynamite	Vibroseis (45-6 Hz)
Pattern	3 Holes	3 Holes	90 Sweeps/1,000'
GEOPHONES			
Pattern	Inline	Inline	Inline
No. per Station	32	32	84
Group Interval	450'	450'	440'
Spread	5400-450-0-450-5400	5400-450-0-450-5400	6600-2640-0-2640-6600
INSTRUMENTS	Analog	Analog	Analog
Field Filter	20-20-100 Hz.	20-20-100 Hz.	6-45 Hz.
Record Length	5.0 sec.	5.0 sec.	17 sec.
Sweep Length	-----	-----	13 sec.
Type of Gain	AGC	AGC	AGC
FOLD	12 Fold CDP	12 Fold CDP	10 Fold CDP
NO. OF CHANNELS	24	24	20

TABLE 2.

Summary of Seismic Field Parameters.

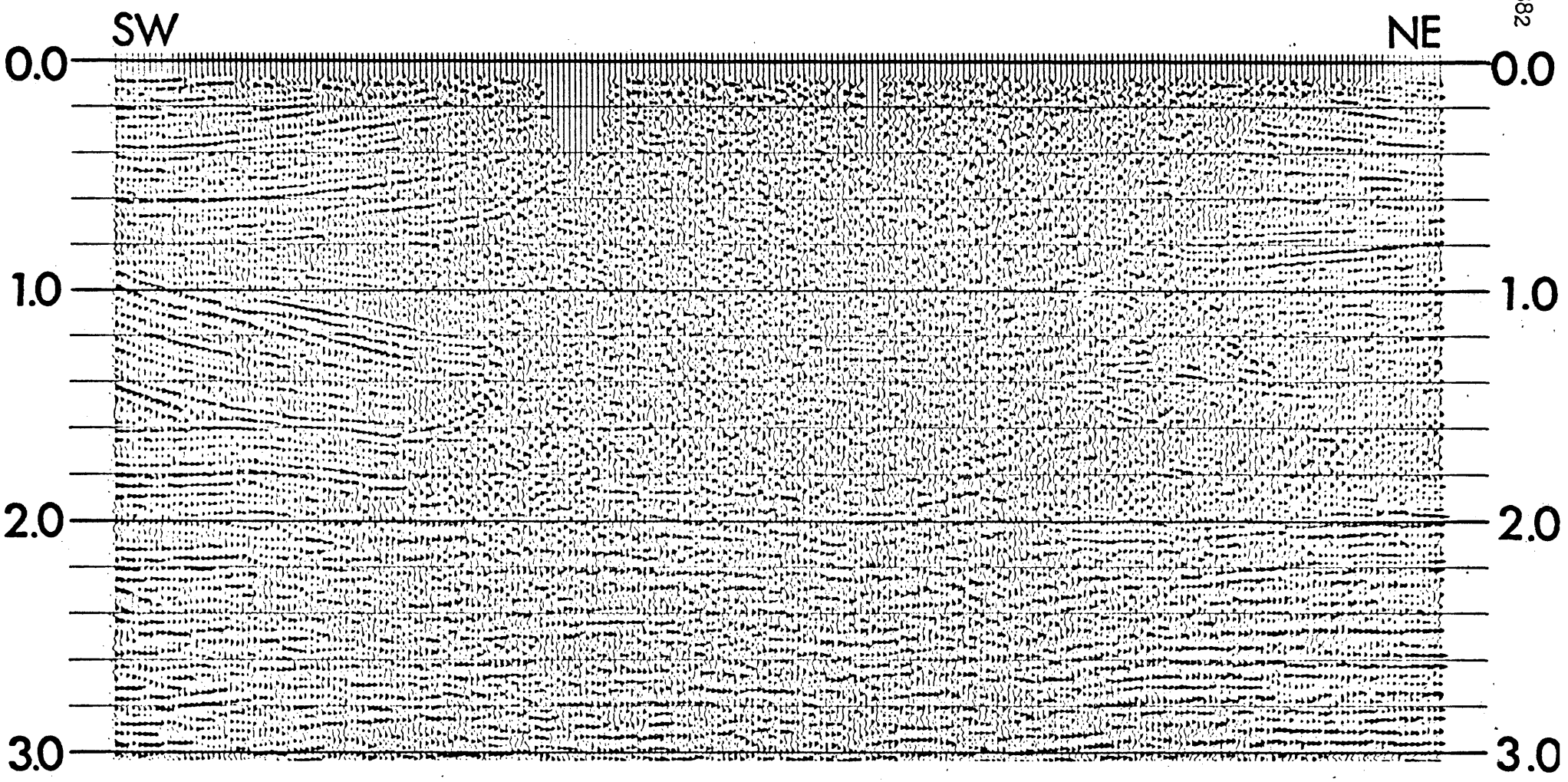

FIGURE 4.

Section A

3 Kilometers

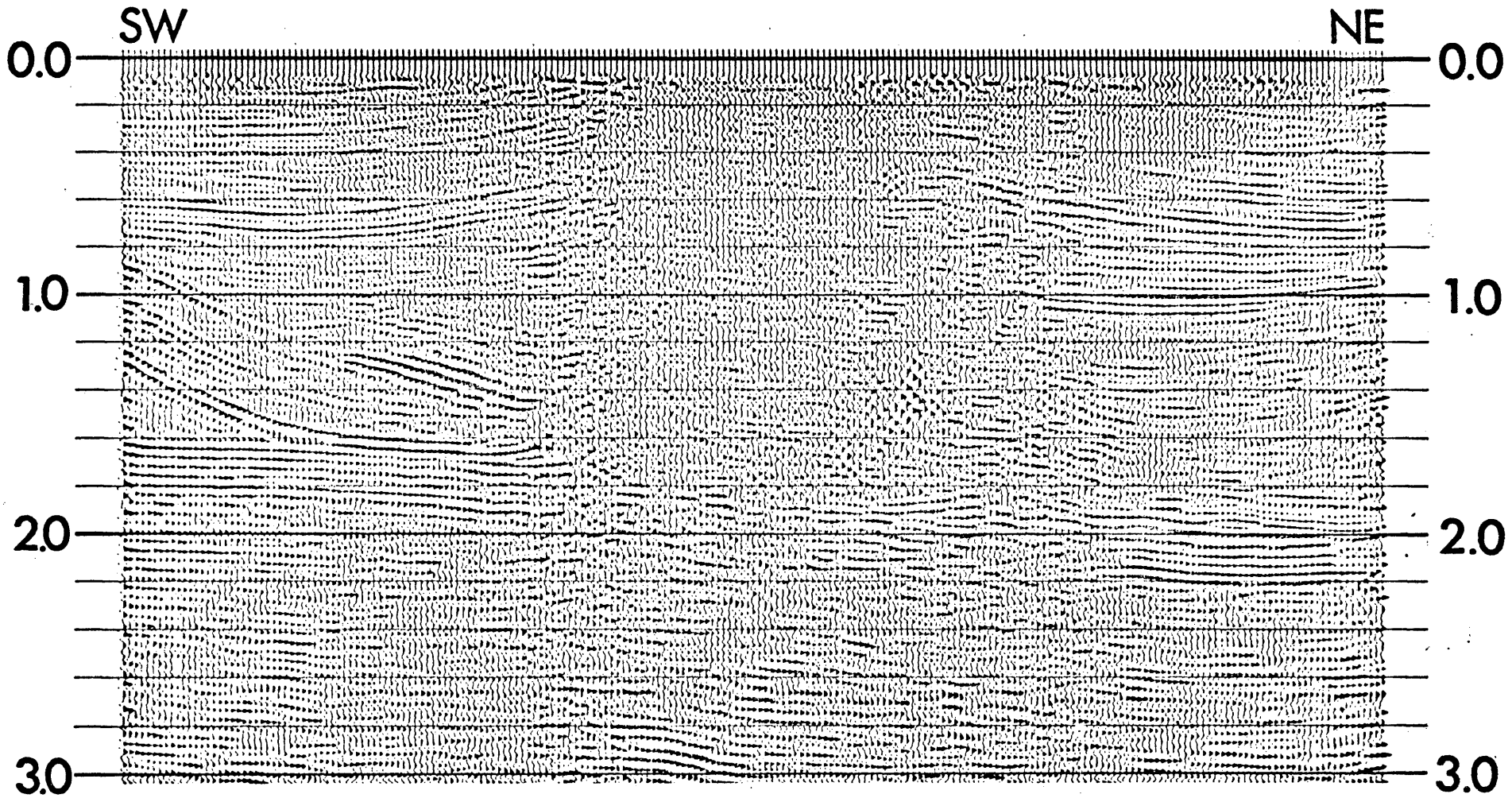

FIGURE 5.

Section B

3 Kilometers

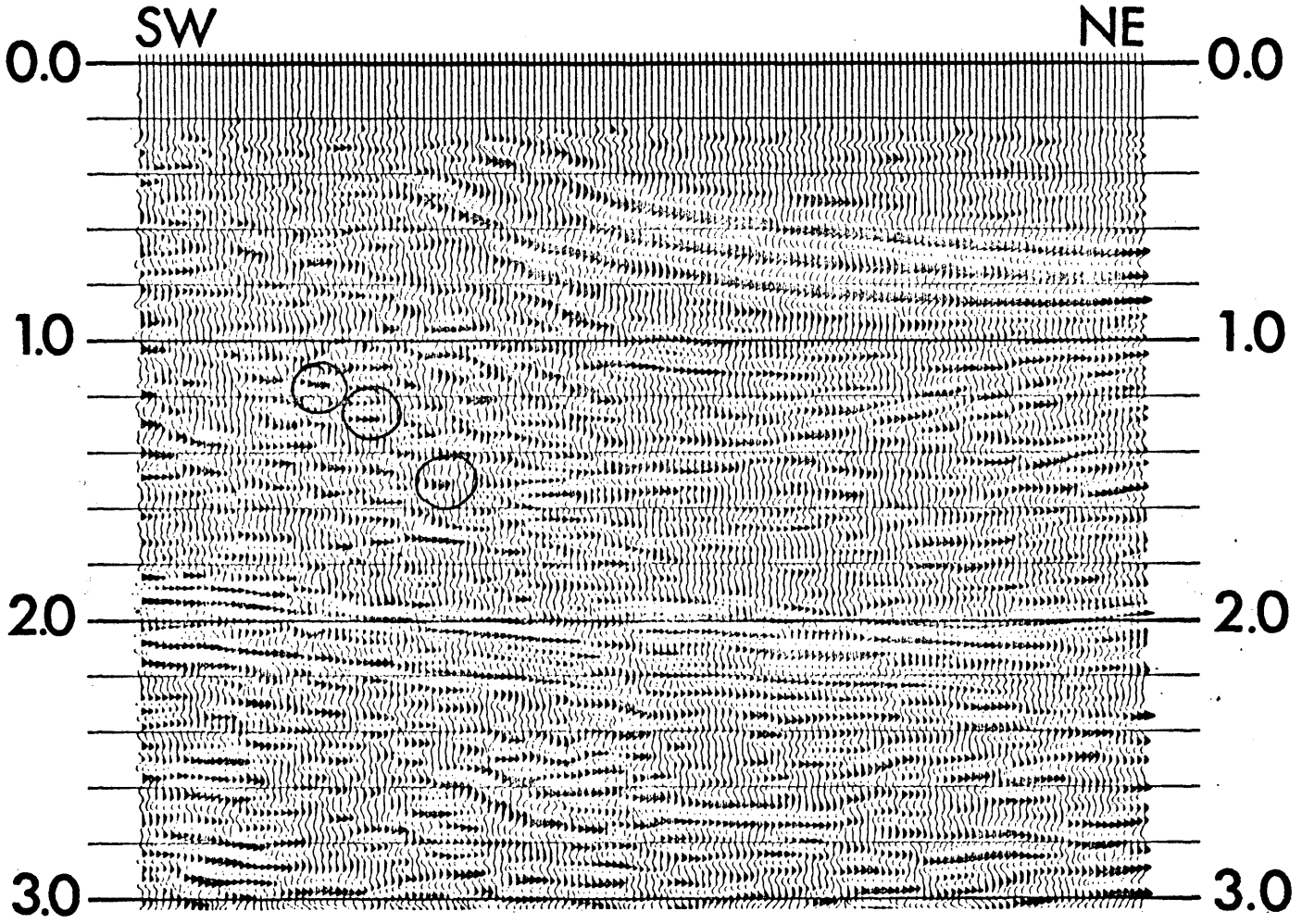

FIGURE 6.

Section C

Circles represent areas where short segment, en echelon seismic events appear.

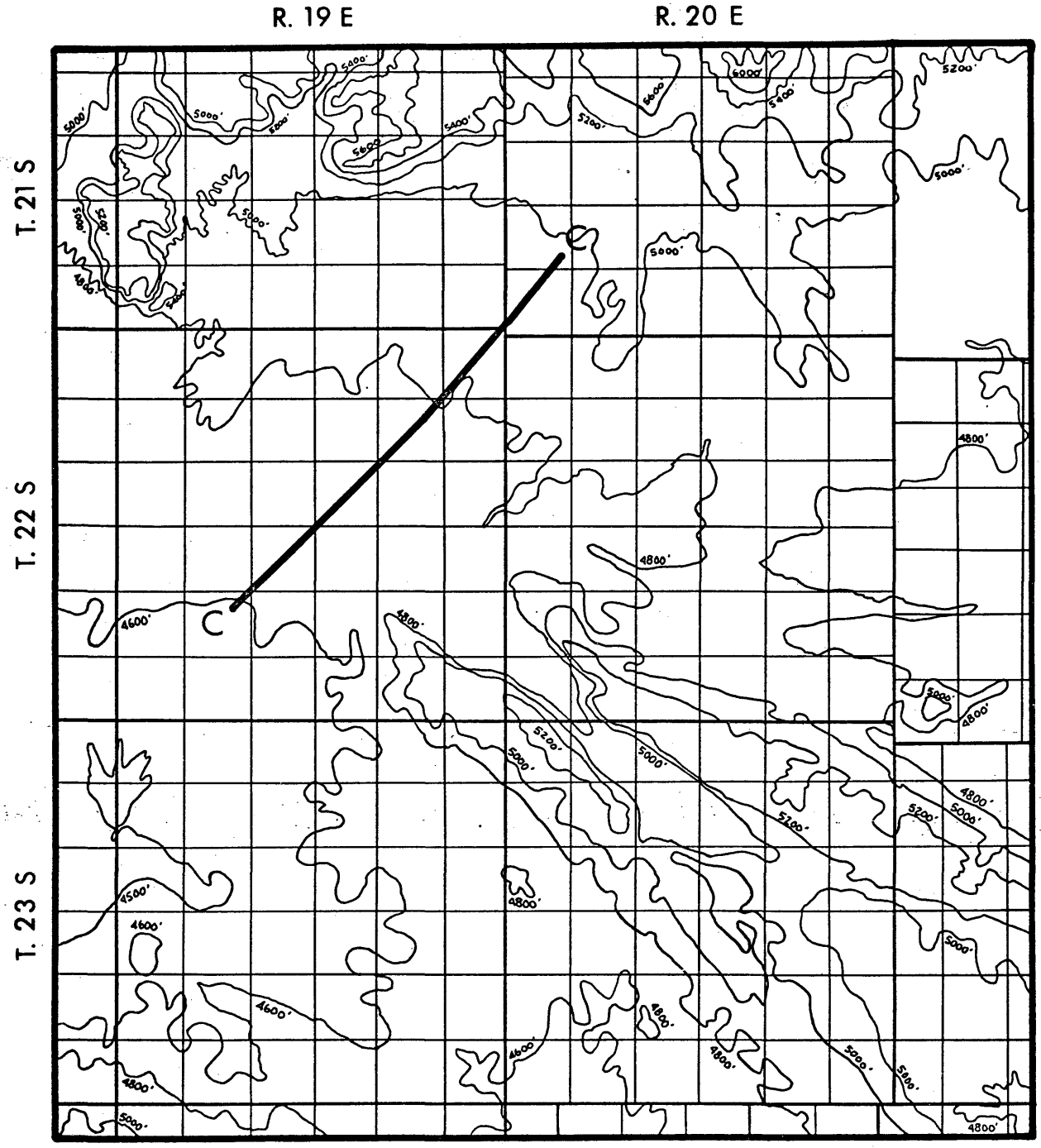

FIGURE 7.

Location of seismic profile C over Salt Valley anticline, Grand County, Utah. Topographic contour interval: 200 feet.

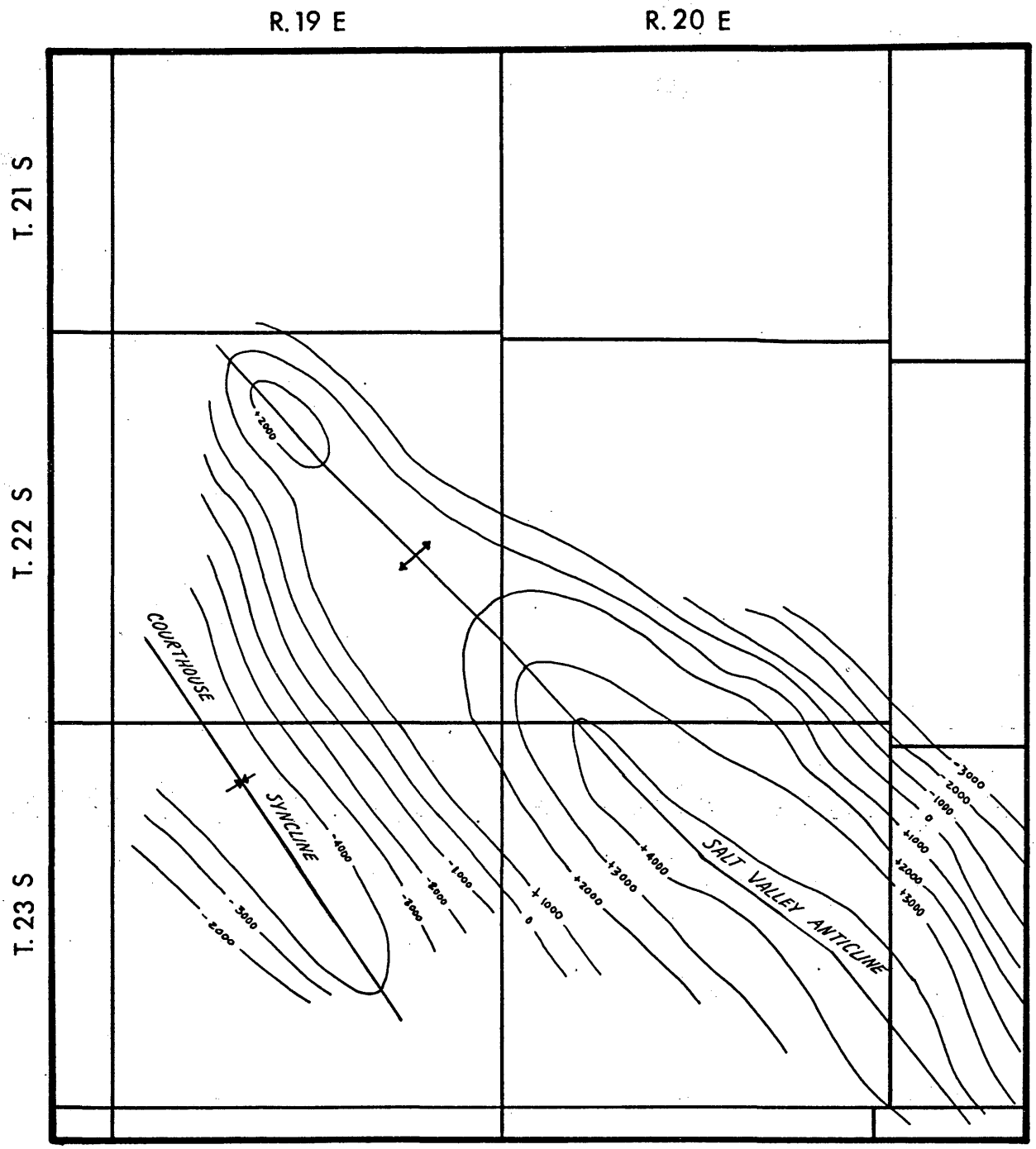

FIGURE 8.

STRUCTURE CONTOUR MAP
TOP OF PARADOX SALT
Salt Valley Anticline

(after Hite and Lohman, 1973)

(Fig. 7 and Fig. 8). The low frequency, band-limited appearance of the seismic data is a result of having used a 45-6 hertz Vibroseis* sweep as a source. This limits the frequencies observed to this narrow pass band (Geyer, 1970). It is obvious from the clarity of the Mississippian acoustic basement that the graben structures at the base of the salt were the primary target area. Lack of resolution of closely spaced events in the shallower section is evident throughout the profile; the edge of the salt diapir is poorly defined. The length of the geophone spread as well as the distance to the near trace (over 800 meters) on Line C further suggests that this seismic profile will be of limited value in the shallow resolution of intra-salt structure, but will provide an excellent diagnostic tool in analyzing the growth history of the Salt Valley anticline in the light of regional tectonics.

Sections A (Fig. 4) and B (Fig. 5) were recorded using dynamite as a source. The broad band nature of this impulsive source is readily apparent and mapping of very shallow (150 to 300 meters), very thin (less than 50 meters) reflectors is possible. Shallow reflections on the flanks of the salt are clearly defined. A major disadvantage of the use of dynamite or other high-energy impulsive seismic sources is the inherent lack of control of the exact frequency and phase character of the source. This depends on ground coupling, charge size, depth and type of source.

*Trademark of Continental Oil Company

Seismic Data Processing

Extensive analysis of the seismic data was performed in order to establish the processing parameters and sequence shown in Fig. 9.

Fig. 10a shows an amplitude spectrum and autocorrelation (Anstey, 1966) of a selected trace from Line C. Several of these analyses were used in determining the optimum deconvolution parameters and as a quality control check on the effectiveness of the deconvolution in attenuating redundant information on the seismic traces (Lindseth, 1967). Severe 13 hertz ringing is evident on the seismic trace. A deconvolution operator length of .140 seconds, which spanned roughly 1.5 cycles of the autocorrelogram, was selected. This operator was thought to be long enough to attenuate short period redundancies on the data, but short enough to avoid attenuation of closely spaced primary events with similar spectral character. A Wiener-Levinson algorithm (Levinson, 1947) was used to calculate the optimum least-square inverse filter. The results, as observed in the frequency analysis of Fig. 10b, show excellent spectral whitening and attenuation of the 13 hertz ringing. There are still some longer period redundancies, but common-depth-point stacking should effectively reduce the amplitude of these.

After deconvolution and application of a zero-phase modified Ormsby frequency-domain bandpass filter (Lindseth, 1967), a spectral velocity analysis was performed at close intervals along each profile in order to determine the optimum stacking velocities. The contoured result of one analysis is shown in Fig. 11. This analysis applies the hyperbolic normal moveout equation to the seismic data as follows:

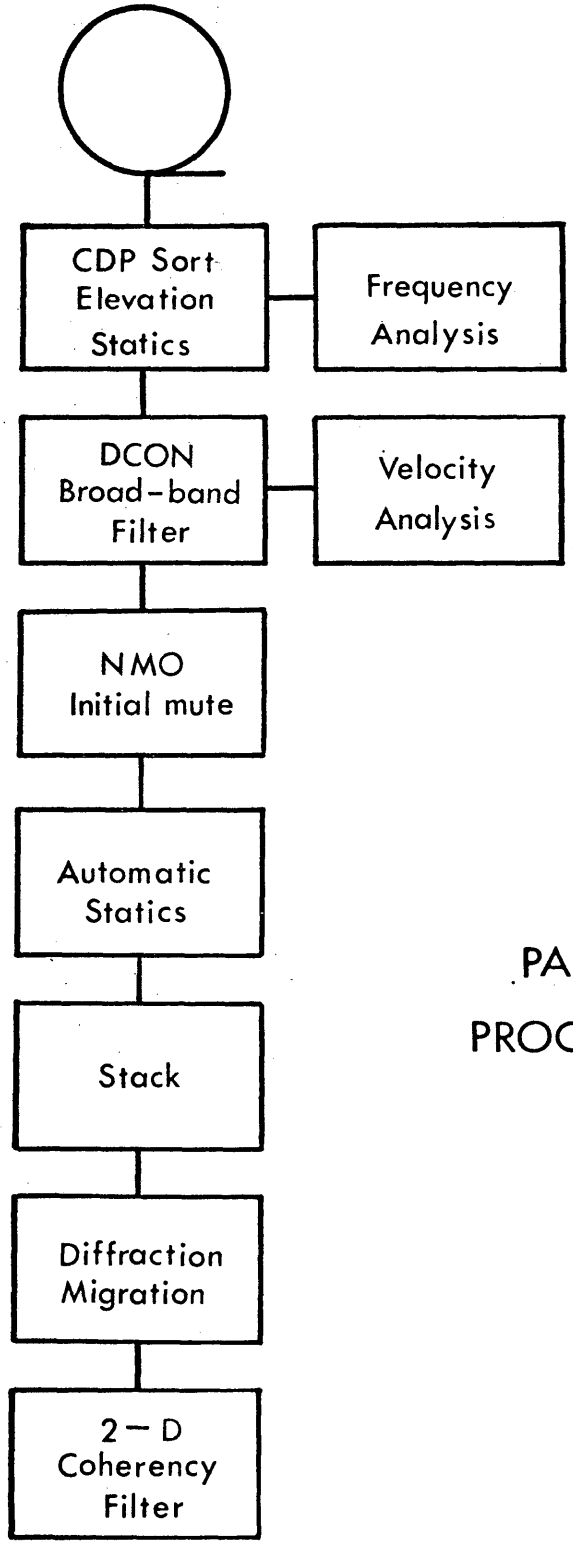

FIGURE 9.
PARADOX BASIN
PROCESSING SEQUENCE

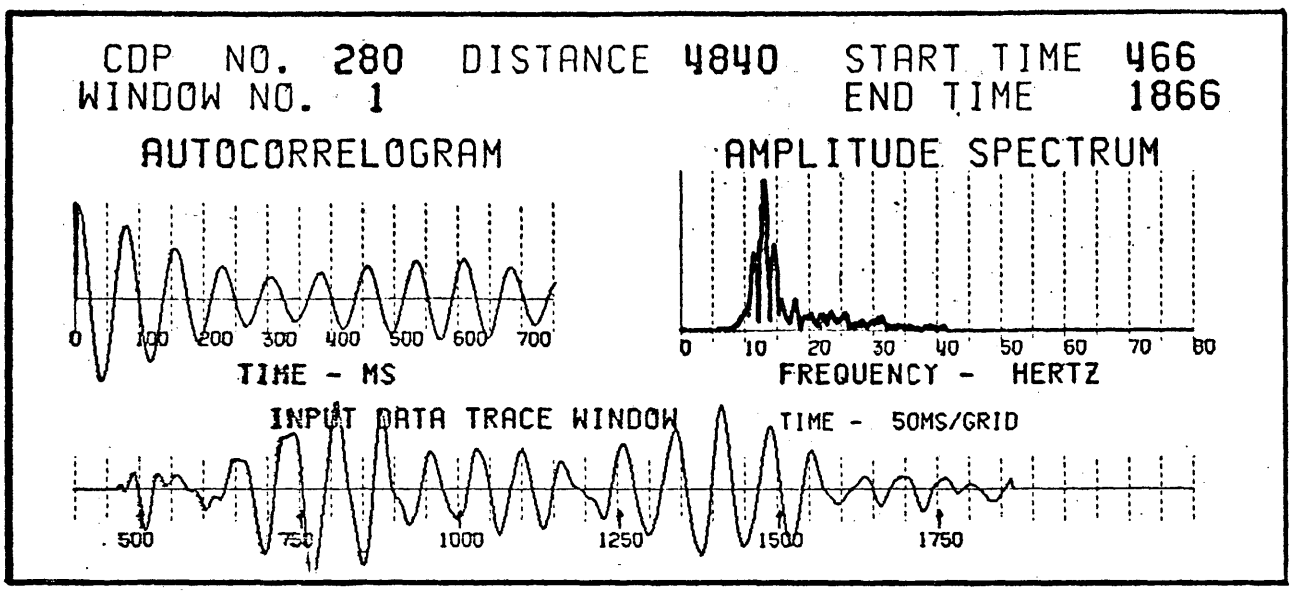

FIGURE 10A.

FREQUENCY ANALYSIS BEFORE DECONVOLUTION

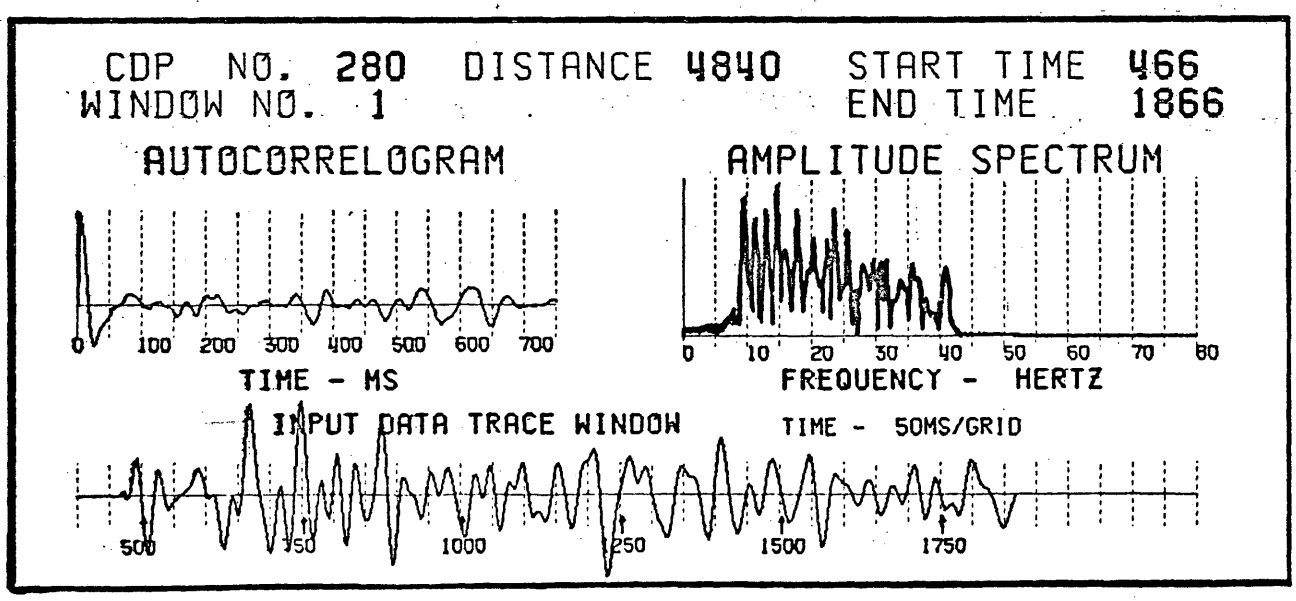

FIGURE 10B.

FREQUENCY ANALYSIS AFTER DECONVOLUTION

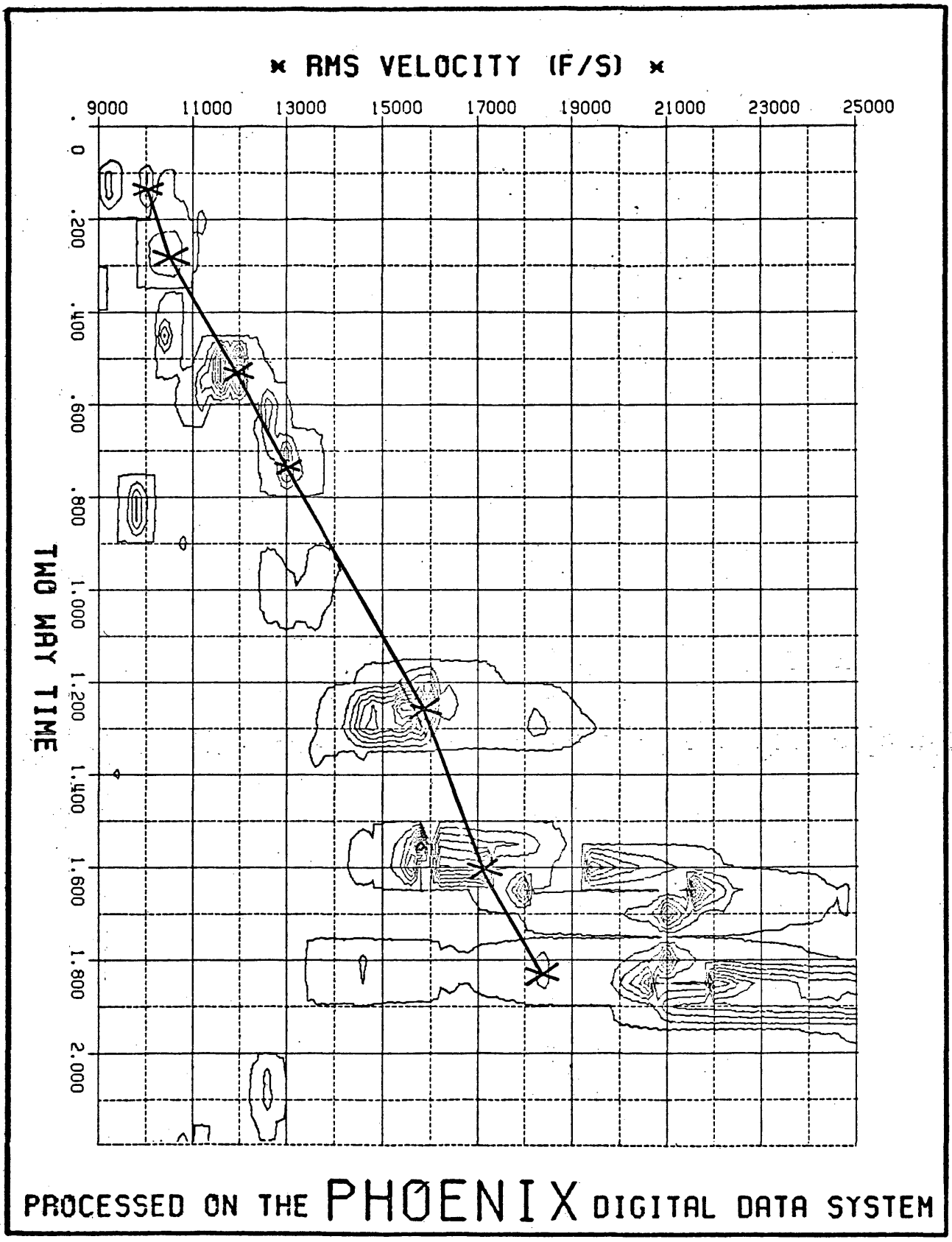

FIGURE 11.
CONTOURED SPECTRAL VELOCITY ANALYSIS

$$\Delta T_{ij} = (T_o^2 + X_i^2/V_j^2)^{\frac{1}{2}} - T_o$$

where: ΔT_{ij} = The time-of-arrival difference between a seismic reflection detected at a receiver at X_i offset from the source and the same event detected at zero offset from the source.

T_o = The two-way travel time of a reflected seismic wave detected at the source.

X_i = The offset from the source of the ith detector.

V_j = The trial stacking velocity (Slotnick, 1936).

The data from a group of common depth points (CDP's) is corrected for normal moveout (NMO), summed (stacked), and then analyzed within small time windows for the maximum power. The results, as seen in Fig. 11, are relative power contoured on an abcissa of velocity and an ordinate of two-way travel time. The analysis is labeled "RMS VELOCITY" (root-mean-square velocity) although it must be emphasized that the velocities represented here are rms velocities only if there are no dipping reflectors and if the rocks behave in a perfectly elastic manner. This misnomer has been accepted in common use throughout the geophysical industry. However, it should be emphasized that this type of analysis yields only stacking velocities. The rock velocities can be approximated via Dix's equation (Sheriff, 1973) after correction for dip. For parallel, dipping layers in the subsurface:

$$V_{rms} = V_{nmo}\cos\alpha$$

where: V_{rms} = The true, root-mean-square velocity (velocity from a flat,

multi-layered, elastic medium).

V_{nmo} = The optimum stacking velocity.

α = The angle of dip of the reflectors in the plane of the seismic section.

For non-parallel, dipping reflectors, as in the Salt Valley anticline, the relationship between stacking velocities and rock velocities is much more complex and must be derived by a downward continuation technique (Claerbout, 1976), or heuristically by ray trace modeling.

Once a velocity-time function was determined for each control point along the profiles, normal moveout corrections were applied to the data in order to correct for varying source-receiver offsets and obtain the maximum power CDP average or stack for all recorded times. As can be seen from the NMO equation, larger ΔT's will occur at smaller T_o's. The distortion due to "stretching" of the far data traces at shallow times was zeroed in order to preserve shallow reflections on near traces in the CDP stack.

Variations in the near surface, or weathering layer - both in thickness and velocity - can often introduce time shifts (static shifts) on the recorded trace, which are not completely accounted for by correction to datum based on the surface elevation of the geophone and source stations. For this reason, in areas where near-surface layer characteristics are not accurately known, a processing technique known as automatic residual static corrections can be used to statistically derive the remaining time shift in the data and "fine-tune" correct the data

to datum. The Salt Valley anticline is flanked by several resistant ridges and shallow faults. In addition, uncompacted Quaternary fill makes accurate characterization of the near-surface layer difficult. Of the several methods of refining time corrections, a surface-consistant statistical approach was chosen. The basic assumption of this method is that late arriving reflected seismic energy comes from deep (relative to source-receiver offset) reflectors where the angle of incidence is nearly normal. With this assumption, redundancies present in the relative time shifts at each source and receiver location can be used to extract a residual time correction for each location along a seismic profile. Fig. 12 shows rays emanating from a common source, but received at different surface locations. Since the reflector is deep, both the downward and the upward travelling raypaths are nearly vertical. However, the downward travelling path through the weathering is nearly the same for all rays; the upward paths are different. Therefore the residual reflection time differences for traces from a common shot can be attributed to near surface effects at the receiver locations and subsurface structure. Likewise, data from common receivers can be assumed to contain time differences due to near-surface effects at the shots and structure. The structure is normally lower frequency and can be separated from the residual statics with a high-pass K-domain filter. Then, a matrix solution for the residual static correction at each point along the profile can be computed. After automatic static corrections, a 10-fold multiplicity stack was performed on Line C; 12-fold stacks

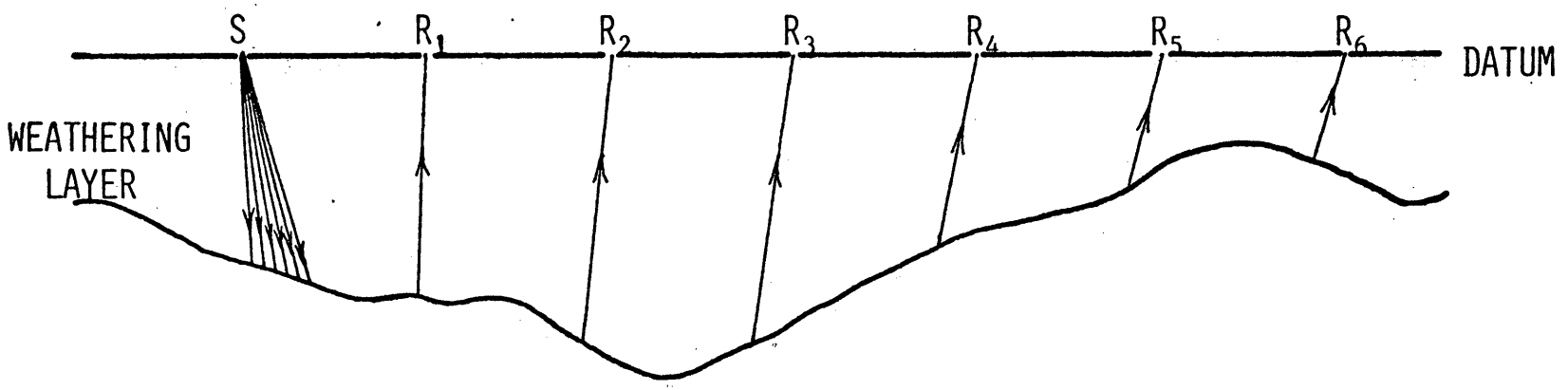

FIGURE 12.

AUTOMATIC RESIDUAL STATIC CORRECTIONS.

Rays shown are from a reflector at a depth of only ten times the geophone interval. The downward travelling path for all rays through the weathering layer is nearly equal so that arrival time differences can be attributed to weathering variations at the receivers.

were performed on Lines A and B.

When seismic data are derived from steeply dipping reflectors, as is the case in the Salt Valley anticline, the time representation cannot be directly converted to depth. This is because each seismic trace represents the sum of a series of depth/velocity vectors which are displayed vertically under a fixed surface location. Most geophones used in conventional seismic exploration are designed to measure only the vertical component of the seismic wave velocity rather than the direction of wave propagation. Furthermore, a sudden velocity or density contrast in the subsurface can disperse (diffract) seismic energy radially in a manner analogous to that observed in elementary optics. The result of this point diffraction of energy is that subsurface points, where this velocity or density contrast occurs, behave like secondary sources (Fig. 13a). According to Huygen's Principle, all reflectors behave like an infinity of point diffractors (Sheriff, 1973). The function then, of the diffraction migration process, is to collapse the dispersed energy back to its point of origin in the seismic time section. Since the diffracted energy "originates" at a point and is received at a line (the surface of the ground), it is hyperbolic in shape. The exact shape of the hyperbola is a function of the wave-front velocity, but in practice, the stacking velocities are a fair approximation to the velocities needed to correctly migrate the data. It can be seen schematically in Fig. 13b that the dipping reflectors will tend to appear steeper, and that closed structures will exhibit tighter closure after migration.

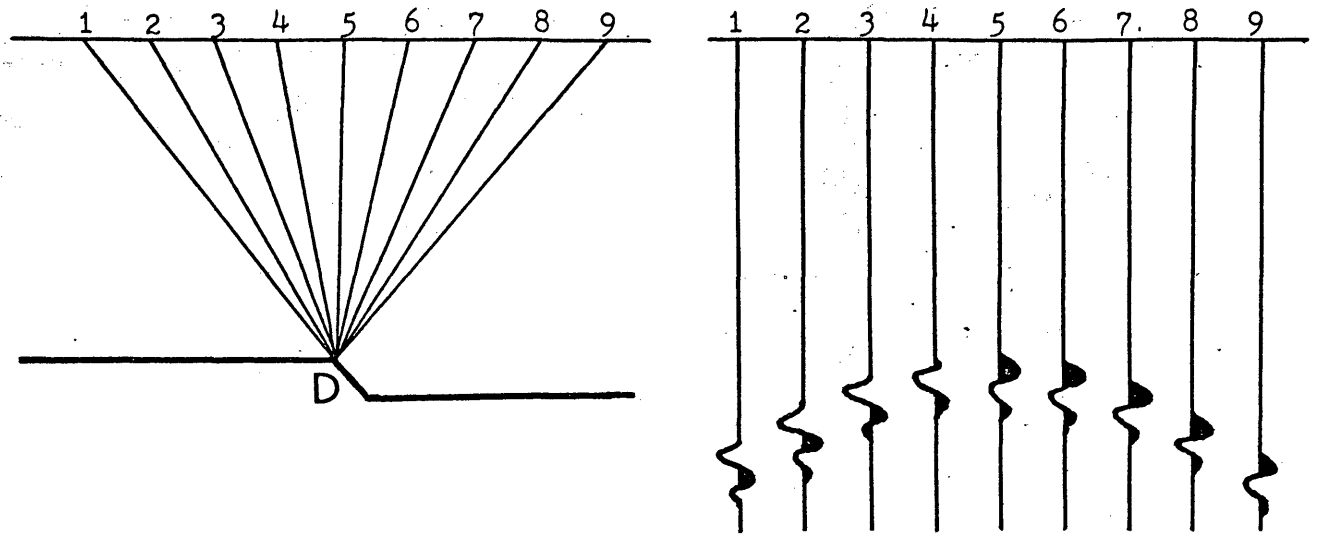

FIGURE 13a

Depth section with sharp acoustic contrast at D diffracting seismic energy in all directions.

Corresponding seismic time profile.

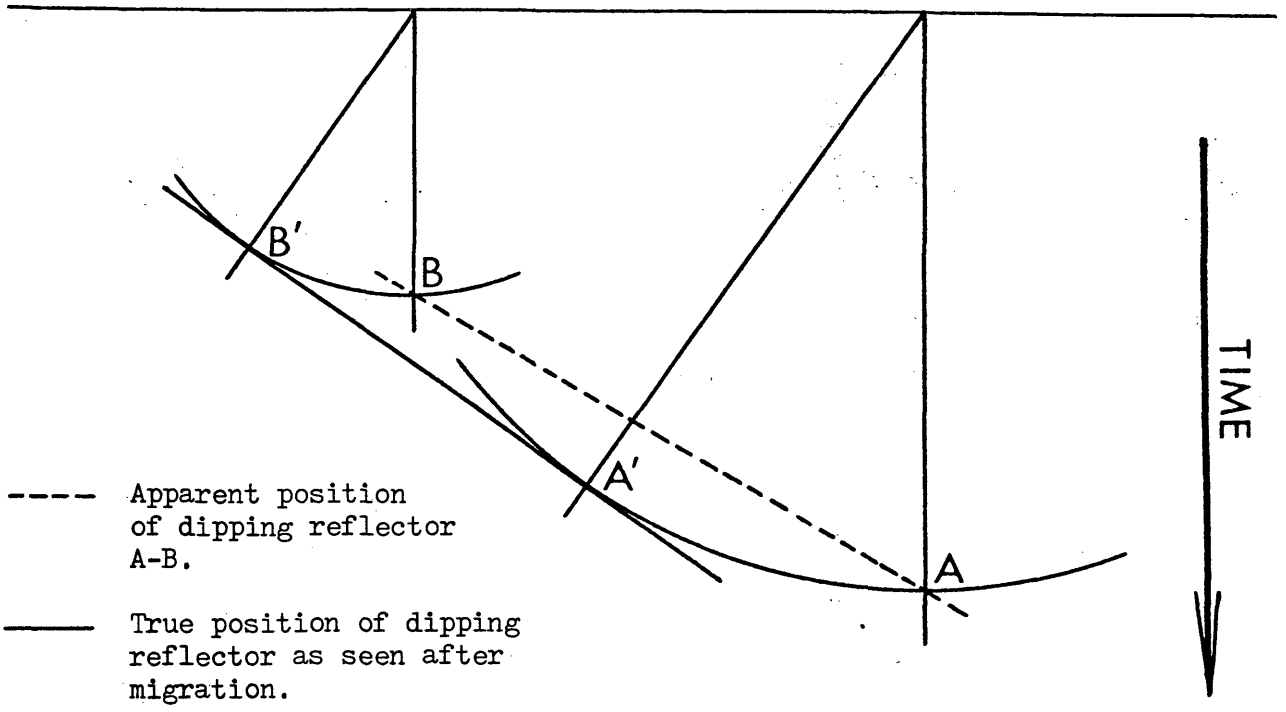

Migration of dipping seismic events.

FIGURE 13b

A two-dimensional ω-k (frequency-wave number) filter was run on the stacked, migrated sections as a final step to improve the signal-to-noise ratio. A two-dimensional Fast Fourier Transform is taken over a portion of the data:

$$\Psi(\omega,k) = \sum_{t=0}^{n} \sum_{x=0}^{m} f(t,x)\exp(-j(\omega t + kx))$$

where: t = The sample number of the seismic trace.

n = The total number of samples per trace less one.

x = The spatial coordinate of the seismic trace expressed as trace number.

m = The total number of seismic traces spatially transformed less one.

f(t,x) = The original data (time-space series).

Once the data are transformed, the amplitude spectra in the frequency-wave-number domain are squared and normalized within a 16-bit computer word. This process effectively eliminates events whose time space coherency is such that their spectral components fall outside the dynamic range of a 16-bit integer computer word. The process also emphasizes coherent seismic events while attenuating incoherent events. The inverse transform is then calculated to return the data to its original form. The two-dimensional coherency filter uses an algorithm similar to that of a velocity or fan filter (Treitel and others, 1967), but does not discriminate against dipping events.

Synthetic Seismograms

Of the available wells in the Salt Valley anticline region, no acoustic logs exist in the planes of the seismic sections. However, a deep acoustic log does exist near enough to the seismic profiles to allow a reasonable degree of correlation when projected into the section. This log, which penetrates the Mississippian strata, was integrated to yield an interval velocity versus time function in this borehole. The reflectivity function was convolved with a minimum phase 14-45 Hertz (12 db/octave roll off rate) wavelet to form the synthetic seismogram shown in Fig. 14. This wavelet was selected because it most closely approximated the shot signature from the source used in the acquisition of Lines A and B. The tops of some of the major lithic units were picked on the synthetic based on the corresponding interval velocity function, and associated stratigraphic logs and driller's reports, as well as the expected acoustic impedances for these interfaces. This well, which produced the synthetic in Fig. 14 was not on the crest of the anticline, but should provide stratigraphic control when compared to the seismic sections. A few other shallow acoustic logs were available in the area, but were not of sufficient quality or proximity to the seismic data to warrant inclusion in this paper. This acoustic log synthetic was projected along strike and tied to Line B as shown in Fig. 15. The correlation was relatively good for most times on the seismic data. Discrepancies can be attributed to: phase distortion in the an-

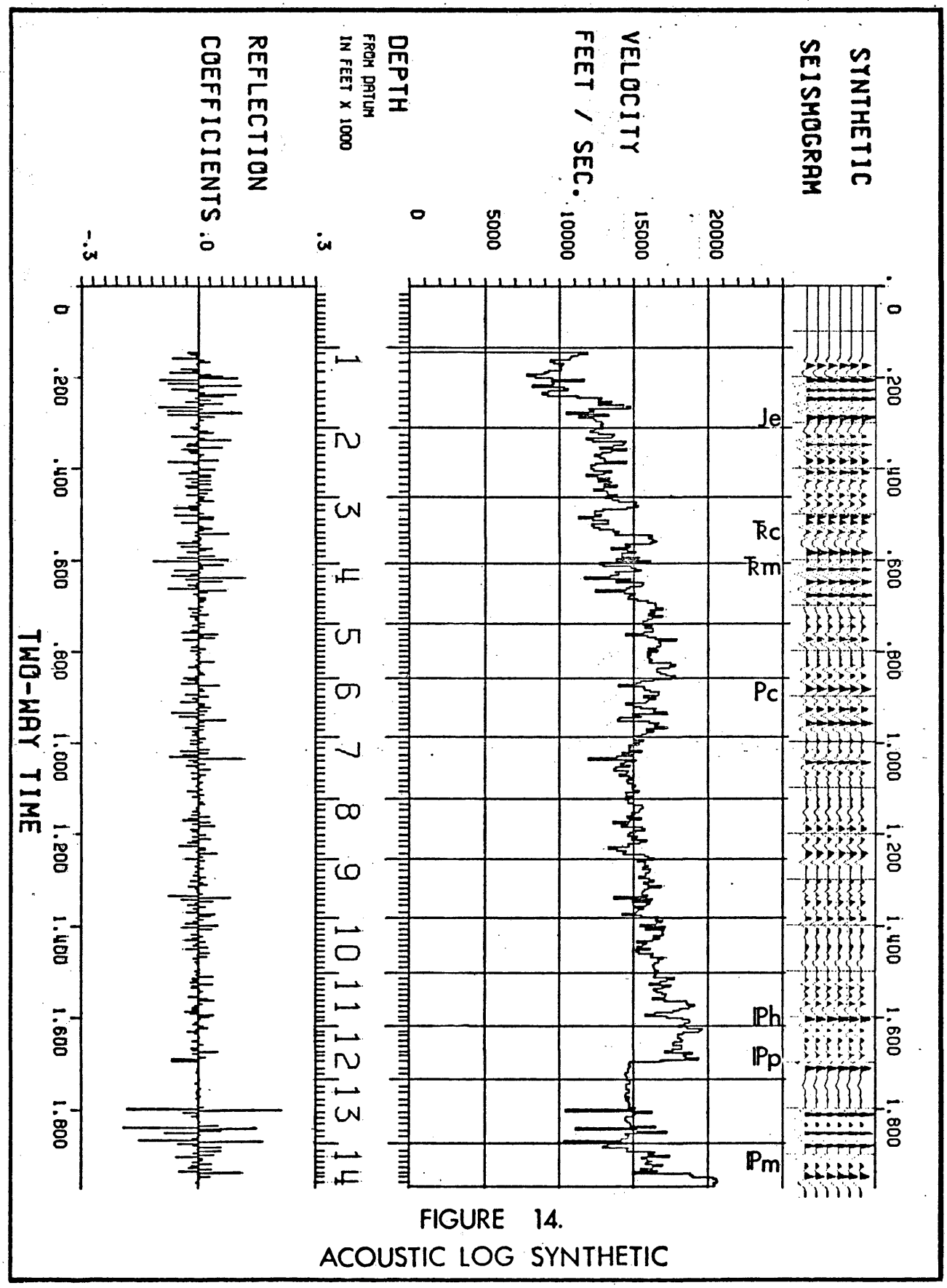

FIGURE 14.
ACOUSTIC LOG SYNTHETIC

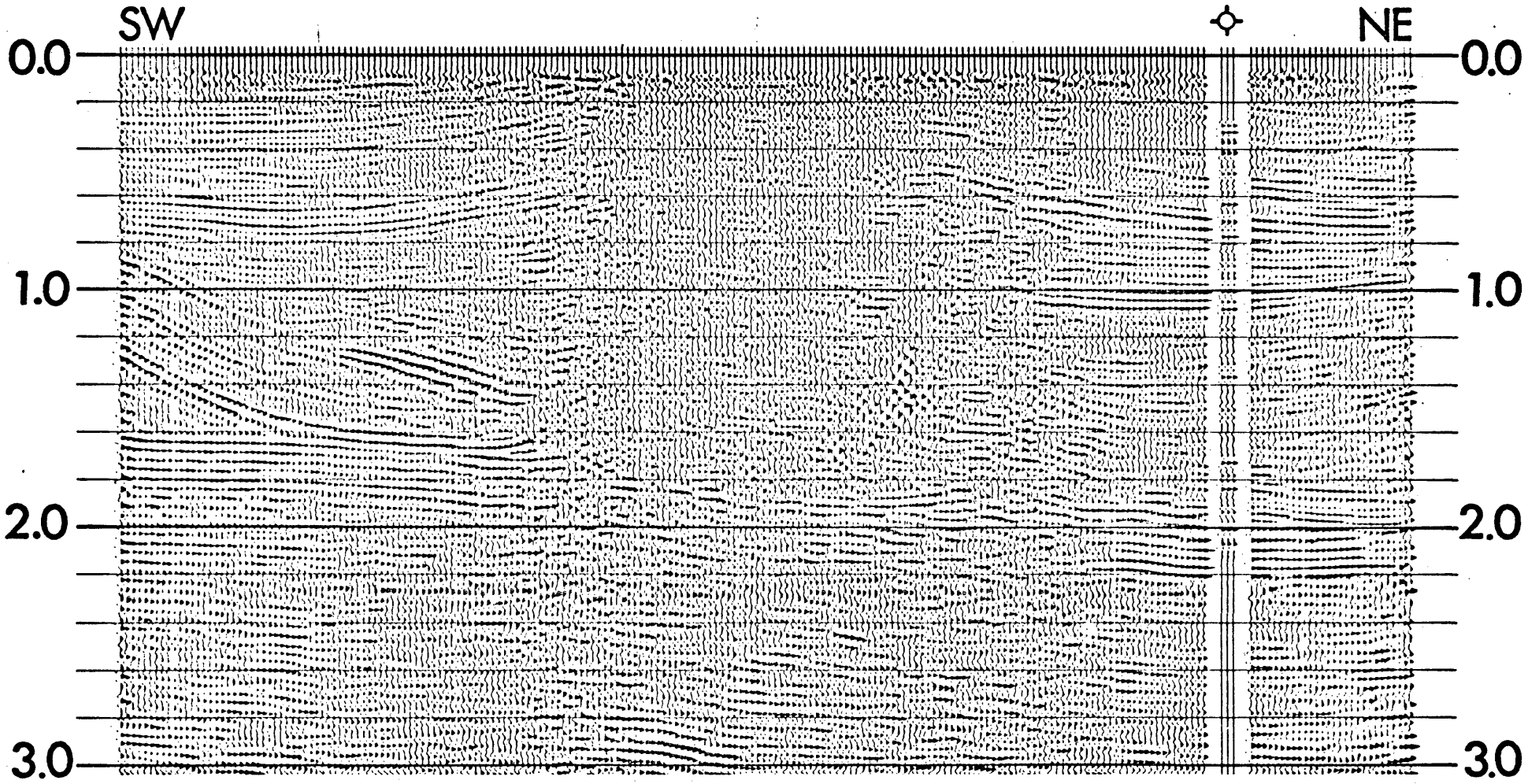

FIGURE 15

Section B with Synthetic Seismogram.

alog field filters used in the acquisition of Line B; spatial variations in the geology; and imperfect resolution of the subsurface on the seismic time section due to noise, multiples, and sideswipe (energy from out of the plane of the seismic section).

INTERPRETATION OF SEISMIC DATA

Fig. 15 shows the approximate correlation between the acoustic log synthetic and the seismic reflection data. This correlation provided the basis for identification of the various reflectors on the seismic sections. This, in turn, allows the interpretation of the growth history of the structure including an analysis of the tectonic control of sedimentation and the relationship between the salt diapir and adjacent structure. Further analysis of the data yields possible characterization of the intra-salt structure. Interpreted sections are presented in Figs. 16, 17, and 18.

Structural Framework

The seismic average velocities in sediments adjacent to the Salt Valley anticline are close to that of pure salt (4,480 meters/second) (Fig. 19), so that little distortion of the Mississippian base-of-salt, due to velocity differentials, can be expected on the seismic time sections. Cater (1970) suggests that salt diapirism was initiated by differential geostatic pressure resulting from an abnormally thick salt wedge being deposited over the downthrown side of the faulted Mississippian basement blocks. The presence of a deep horst-graben system under the salt (Fig. 18) lends credence to the concept of structural influence, if not initiation, of the diapirism. However, the dramatic thickening of flank sediments toward the synclinal axes on either side of the salt

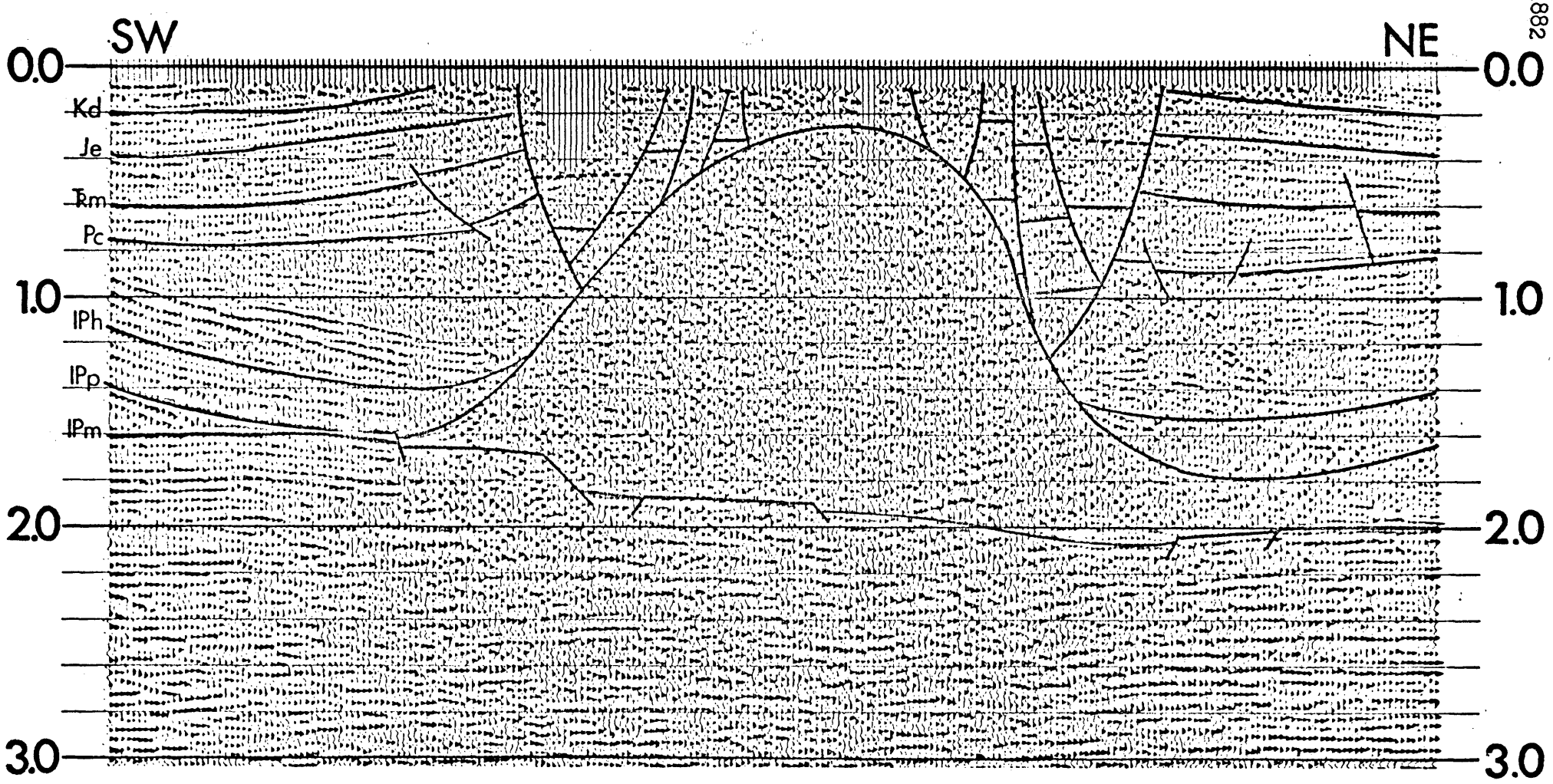

FIGURE 16.

Section A–Interpreted

3 Kilometers

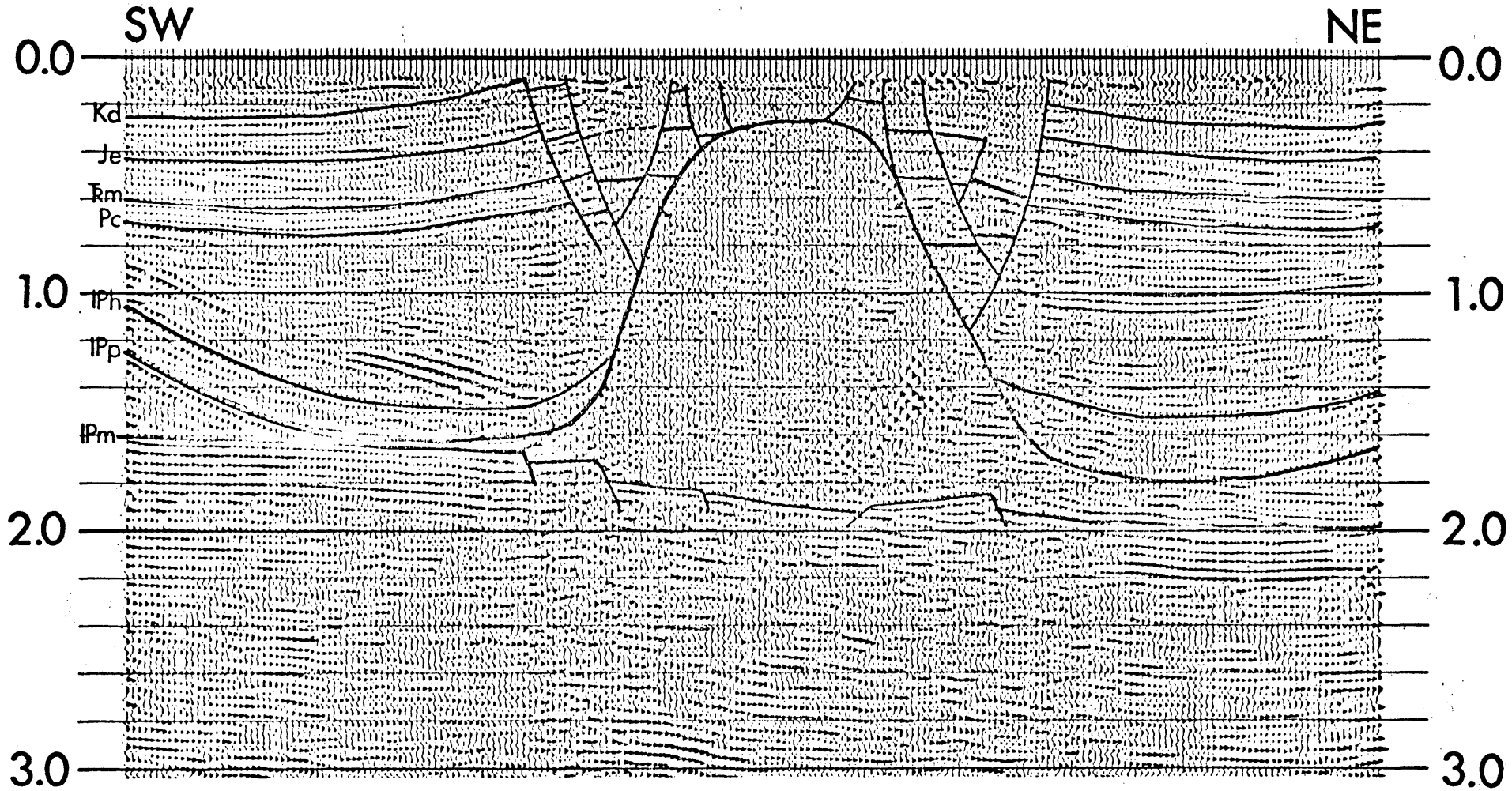

FIGURE 17.

Section B – Interpreted

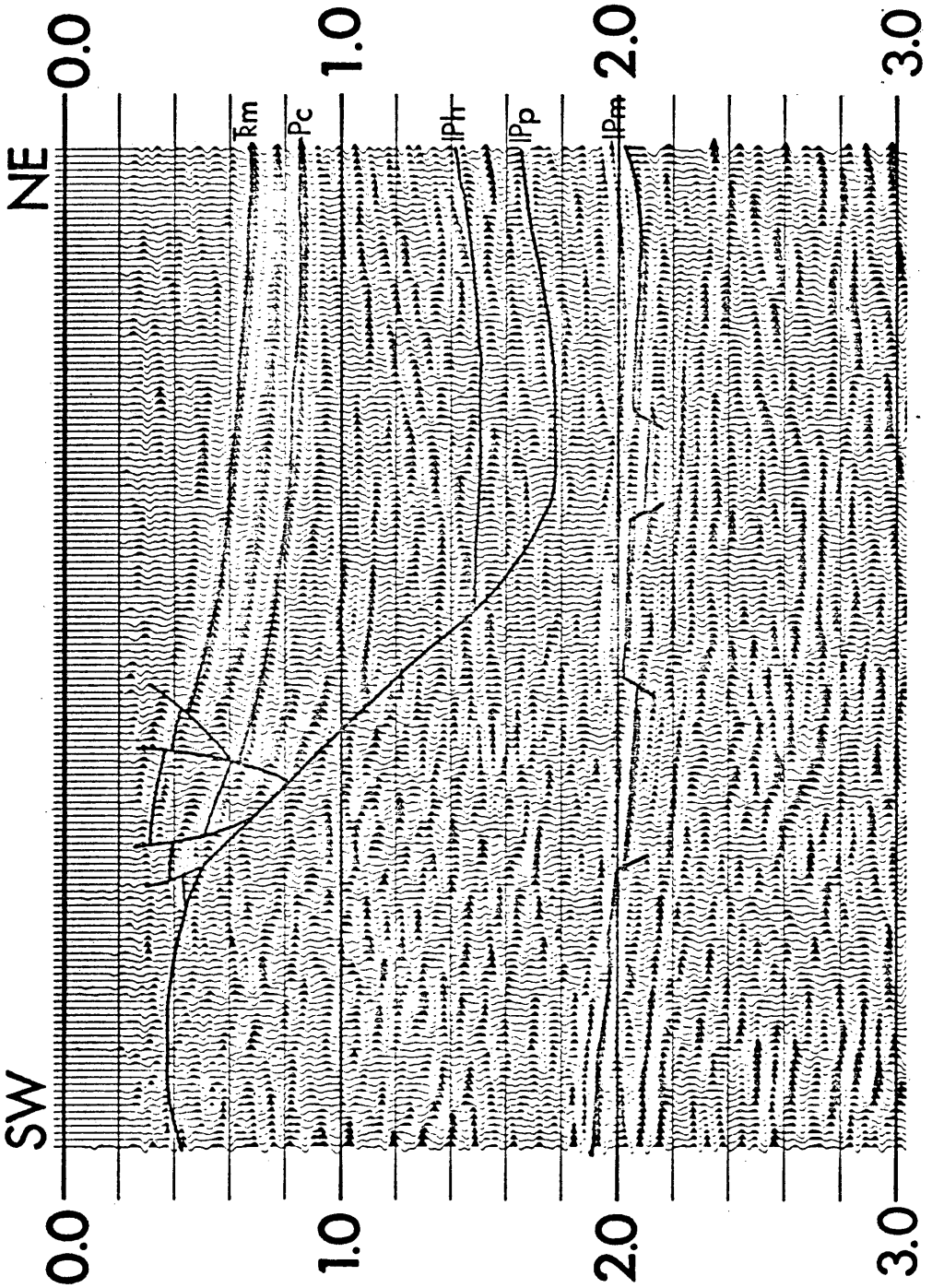

FIGURE 18.

Section C– Interpreted

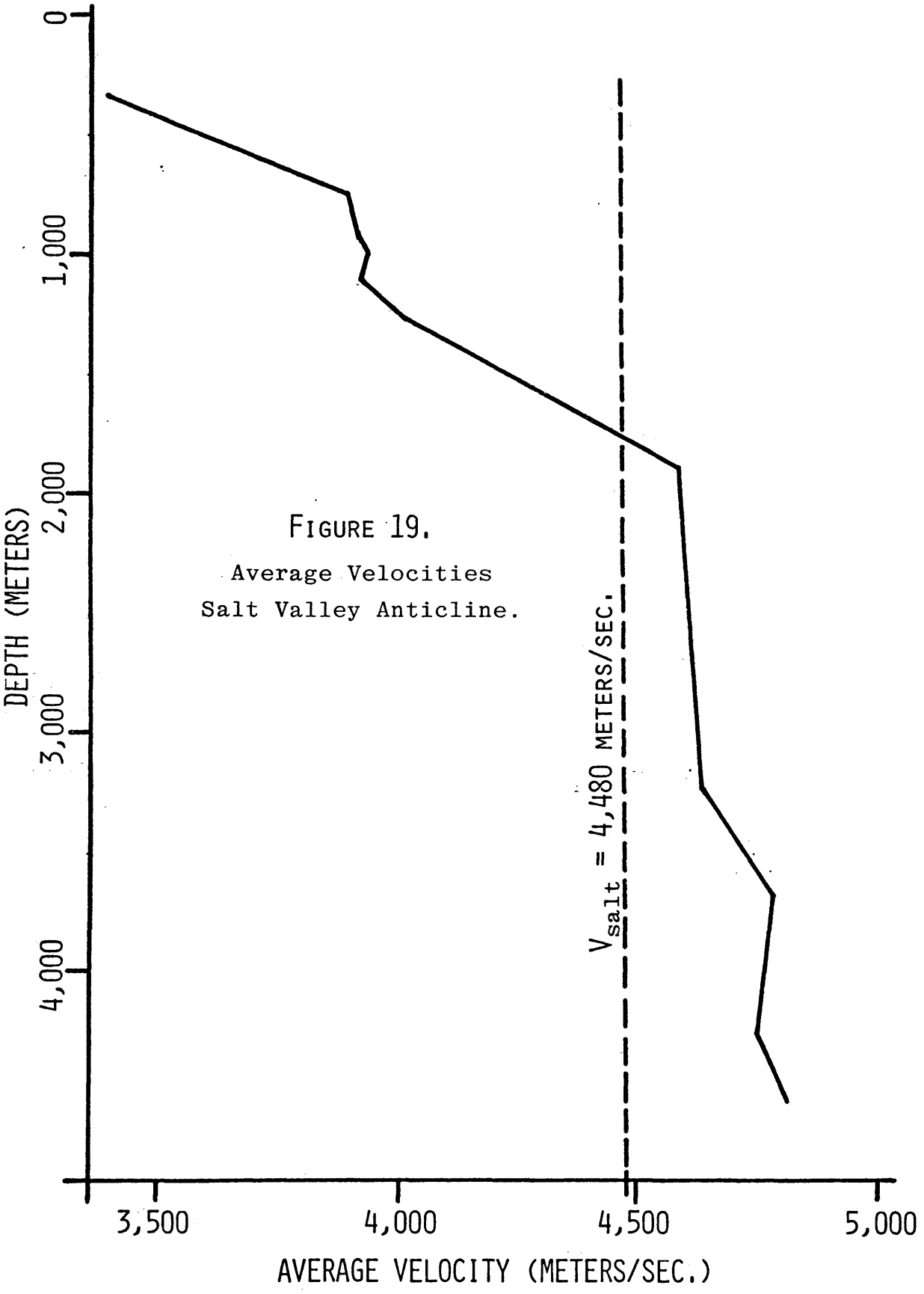

FIGURE 19.

Average Velocities
Salt Valley Anticline.

ridge indicate positive sedimentary control of the upward movement of the halite. Line B (Fig. 17) shows roughly 1.6 seconds of seismic two-way travel time from the top of the salt, which is near the surface, to the base of salt. This time difference indicates over 3,500 meters of salt at the anticlinal axis. This implies approximately the same amount of differential thickness in the adjacent sediments. The saltward thinning of the Hermosa Formation, as indicated on Lines A and B (Fig. 16 and 17), suggests that diapirism had already begun by middle to late Pennsylvanian time. Density contrast and the resultant bouyancy of the salt relative to the surrounding strata have long been accepted as the primary mechanism for diapirism in salt (Nettleton, 1934). Thus, it is apparent that initial salt diapirism was structurally influenced, but that continued rapid sedimentation, associated with the removal of salt from the flanks of the salt swell, maintained the upward momentum of the salt mass. Tanner and Williams (1965) discuss the necessity of regional tension on an axis which is perpendicular to the ridge trend, in addition to a density contrast, in order to effect salt diapirism.

Secondary movement of the basal faults, accompanied by uplift of the Uncompahgre highland, caused an accelerated second-stage growth of the salt swell during the Permian. The Cutler arkosics were deposited during this time in the subsiding basins on either side of the anticline as salt was removed. Continued growth was further accelerated by the migration of the basin axes toward the salt swell as is apparent from the thickening of the Cutler Formation toward the salt. The Permian

sedimentation and saltward thickening has been discussed by Barton (1933) and others as a "down-building" process in which subsidence of flank sediments around a "stationary" diapir is thought to be the predominant structural mechanism. The saltward migration of the depocenter was first explored by Balk (1949).

Third stage salt diapirism is supported by the partial piercement of the younger Cutler arkosics and post-Permian section. The seismic time thinning of the shallower sequence near the crest of the salt on all three seismic sections is indicative of either an interval velocity increase due to compaction of the younger rocks or, more likely, the result of spine movement of the salt occurring faster than Mesozoic sedimentation. It should be emphasized that, although salt flow is divided into three stages, the diapirism was probably continuous. The distinction, then, between the three stages of salt movement is one of degree rather than one of distinct cycles. The transition between the severe structural deformation at the top of the Paradox salt to the milder disruption of the Cretaceous sediments is a gradual one.

Intra-salt Structure

Structure within salt diapirs has been studied extensively by Williams (1961), Biot (1964), Hite and Lohman (1973), Evans and Linn (1970), and others. Most of these authors agree that structural complexity increases greatly toward the axial core of the salt diapir. The distinction between the salt anticlines in the Paradox basin and

those studied in the Gulf Coast, for example, is that the axis of symmetry is planer rather than linear. This symmetry should allow the prediction of a folding character of considerably less complexity parallel to the anticlinal axis (R. J. Hite, oral commun., 1976).

Evans and Linn (1970) mapped in detail the potash, anhydrite, black shale, and dolomite interbeds within the Cane Creek anticline, which lies roughly 40 kilometers south of the Salt Valley anticline, and found second-order assymetric folding with wavelengths up to 120 meters and amplitudes on the order of 25 meters. They also noted third, fourth, and fifth order crenulations with similar assymetry superimposed on the larger folds (Fig. 20). The wavelengths of the smallest folds were on the order of 3 centimeters. They further observed incipient transposition structures in which the nose of a fold had begun to detach from the main structure. This intense folding is the result of lateral and axial compression due to the upward flow of the Paradox salt. The combination of temperature, geostatic pressure, water content, and density contrast of the salt with other constituents caused plastic upward flow relative to the more stable interbeds (Gussow, 1960). Hite (1960) classified nearly thirty distinct marker beds within the saline facies of the Paradox basin. Thicknesses of these beds varies from 5 to 70 meters. Extrapolation of these interbeds northward into the Salt Valley anticline is further complicated by the fact that recumbent folding of some of the markers and near-vertical orientation has caused some of the interbeds to be repeated as many as five times in a single borehole (Fig. 21).

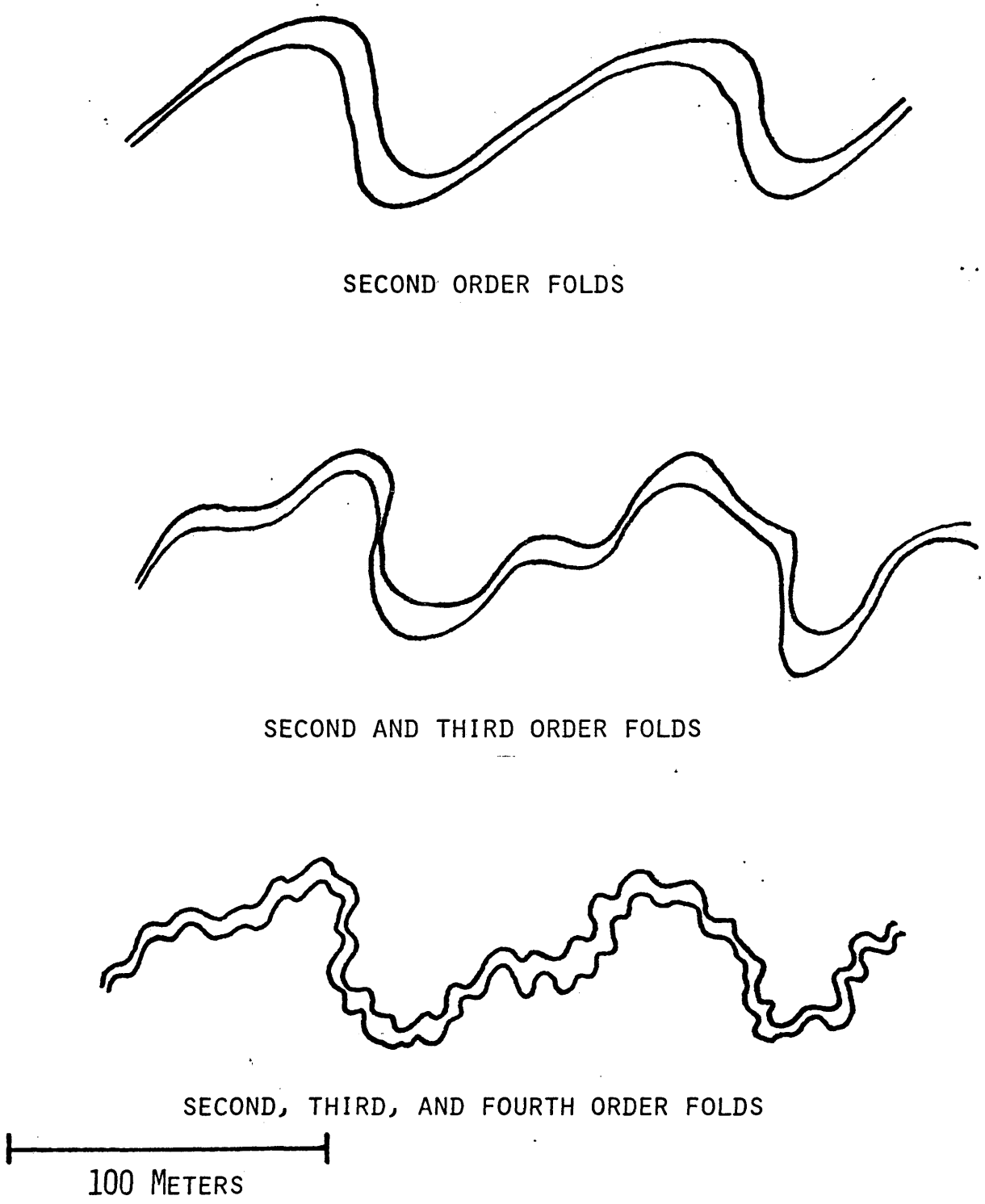

FIGURE 20.

Intra-salt Folding in the Cane Creek Anticline.

(adapted from Evans and Linn, 1970)

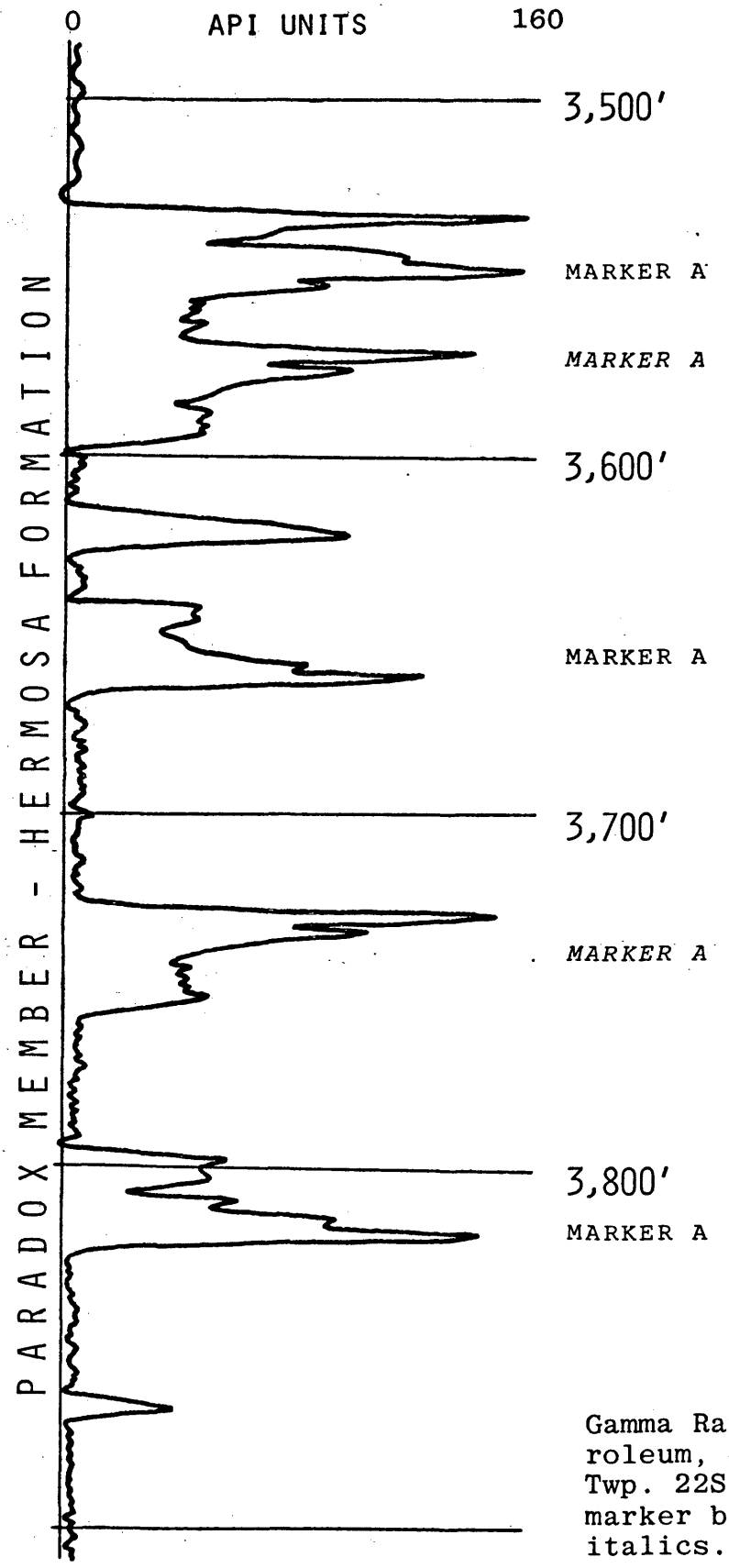

FIGURE 21.

Gamma Ray Log - San Jacinto Petroleum, Salt Valley #3, Sec. 25, Twp. 22S, Rge. 19E. Overturned marker beds are indicated by italics.

The concentration of non-halite clastics and carbonates near the base of the Paradox salt indicate a shallow marine penesaline environment, but also suggest velocity differentials between the upward movement of the impure evaporites and that of the purer halite (Kupfer, 1974). If this were the case, the shallower salt should be purer. This, in fact, is observed in the well data available in the Paradox Member of the Hermosa.

Some coherent seismic events appear within the salt on the processed sections. Line C (Fig. 18) presents one of the best examples of this. Several short iso-time lineups of seismic events are apparent in a general en echelon pattern in the salt. There are no continuous indications of the presence of a reflector in the shallow salt; however, if the folding is of the suspected degree of complexity, these segments could be attached by vertical segments (no reflections) or they could be transposition folds. A similar intra-salt reflection character is evident on Lines A and B although poor signal-to-noise on these sections obscures these reflections. A third possibility for the origin of these coherent seismic events, which will be discussed in more detail in the modeling section of this report, is that the segments represent buried foci due to concave-upward folding of the high acoustic contrast interbeds. In any case, the indications on the seismic sections are, at best, indirect. That is, the exact shape and location of the interbeds is only implied. Since the absence of interbeds, rather than their presence, is of paramount importance for a nuclear waste emplacement site, these indications may provide sufficient evidence to

warrant further study. Higher resolution seismic profiles could provide a more direct indication of the nature of the interbeds. Closer spacing of seismic surface stations would allow better coverage of complex folding in the subsurface and higher seismic frequencies should permit closer definition of reflection time.

COMPUTER SUBSURFACE MODELING

Detection of thin interbeds within salt can be visualized as the mapping of high acoustic impedance layers in a homogeneous, isotropic halfspace. Computer modeling under this assumption was first performed in order to evaluate the pitfalls in this assumption and to selectively account for further complications introduced by complex stratigraphic and structural variations within the subsurface. Fig. 22 depicts two of the simplest variations on the original assumption: that of varying interbed thickness, and that of varying interval velocity. The reflection coefficient for normally-incident seismic rays can be computed as a function of the velocity-density product:

$$R_{12} = \frac{\rho_2 V_2 - \rho_1 V_1}{\rho_2 V_2 + \rho_1 V_1}$$

where: ρ_n = The density of layer n.

V_n = The interval velocity of layer n.

The sign of the reflection coefficient is positive if the energy passes from a lower ρV medium to a higher ρV medium. Normally incident rays are assumed in the modeling because the downward-travelling raypath is coincident with the reflected upward-travelling raypath and because amplitude variations due to mode conversions may be neglected. The deepest layer in Fig. 22 represents a 30 meter thick interbed with a linearly varying velocity ranging from 2,590 meters/sec. (a shale) at the left end to 6,096 meters/sec. (an anhydrite) at the right end. Densities in this

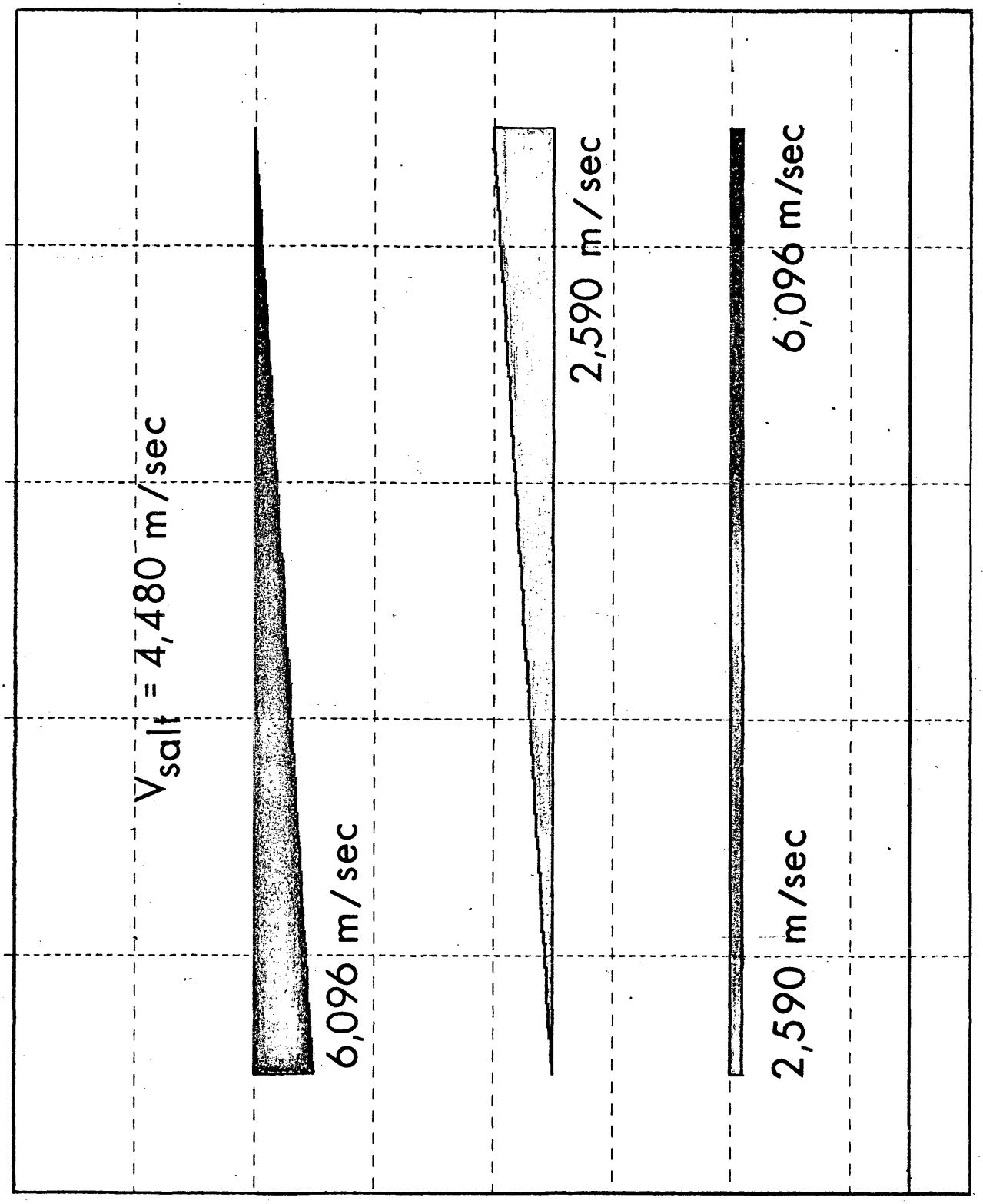

FIGURE 22.

Thinbeds Model with Thickness and Velocity Variations.

model were held at 2.4 grams/cm^3. Fig. 23 illustrates that as this density-velocity product passes through that of salt, the numerator of the reflectivity equation approaches zero and the interbed becomes seismically transparent. This potential difficulty would exist where a facies change in the interbeds or a change in fluid pressure occurred. The top two wedges of high and low velocity material respectively vary from 150 meters to 0 meters in thickness and illustrate one of the resolution problems inherent in mapping closely spaced reflectors. The wavelet used to generate this synthetic section was a minimum phase wavelet with a median frequency of 26 hertz (Fig. 24) (Ricker, 1953). This wavelet closely approximates the impulsive source signature of sections A and B. It can be seen that constructive reinforcement of the wavelet from the salt-interbed boundary with that from the interbed-salt boundary obscures the true nature of the reflectors.

Although the usefulness of conventional reflection seismic methods is limited by the intense interbed folding, the distortion of the interbeds in the salt may provide a promising indirect indication of the presence of interbeds. Fig. 25 shows a hypothetical model of a severely folded thin bed imbedded in a salt-like medium. Buried focusing, as seen by the crossed raypaths (Rieber, 1937), results in the seismic signature shown in Fig. 26. This indication of folded interbeds has the advantage of being relatively independent of interbed thickness. Major disadvantages to this method include the fact that this is an indirect, rather than a direct, method of detecting the presence of interbeds in the salt and the method depends on the geometry

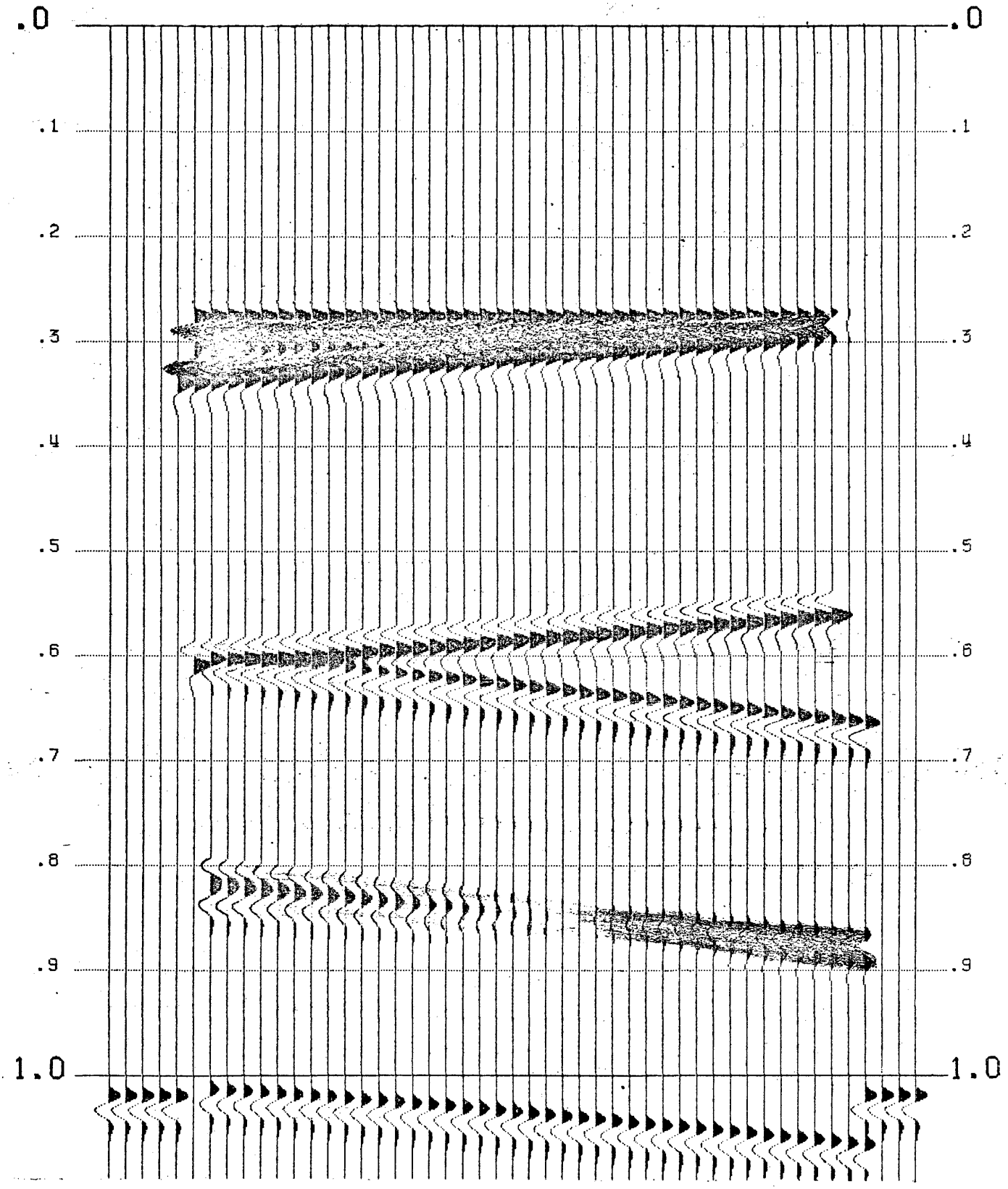

FIGURE 23.

Thinbeds Synthetic Seismic Section.

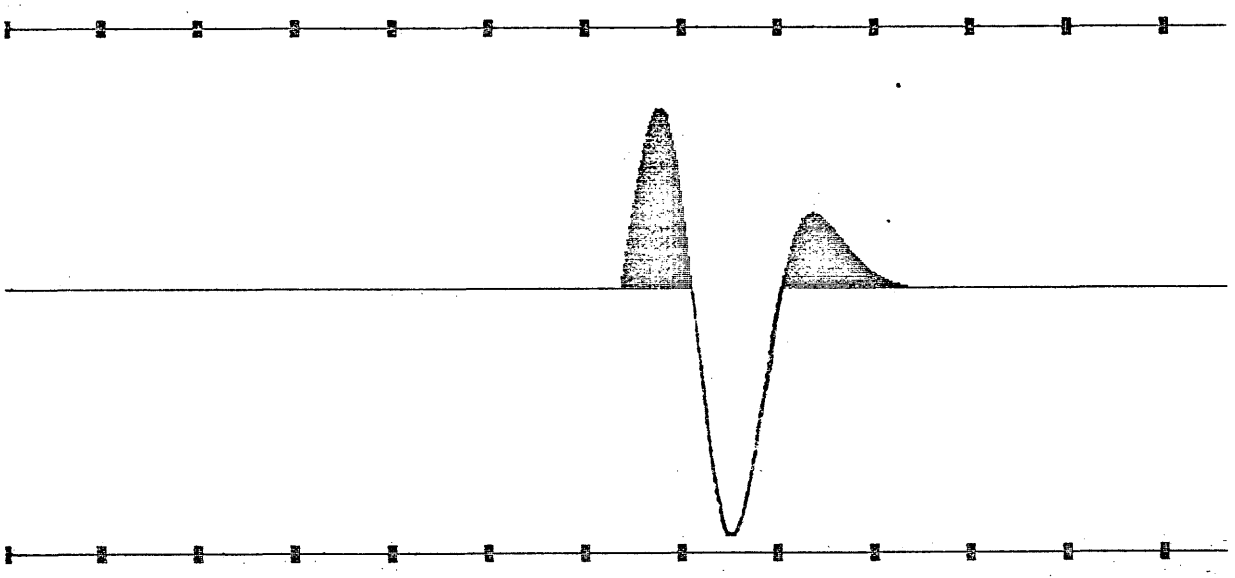

MEDIAN FREQUENCY: 26 HERTZ

FIGURE 24.

Minimum phase Ricker wavelet. The attenuation of this wavelet is proportional to the square of the frequency (see Ricker, 1953). This wavelet is that which would result from an impulsive seismic source with transmission through an ideal viscoelastic medium. This wavelet was used in the generation of all synthetic sections shown in this paper.

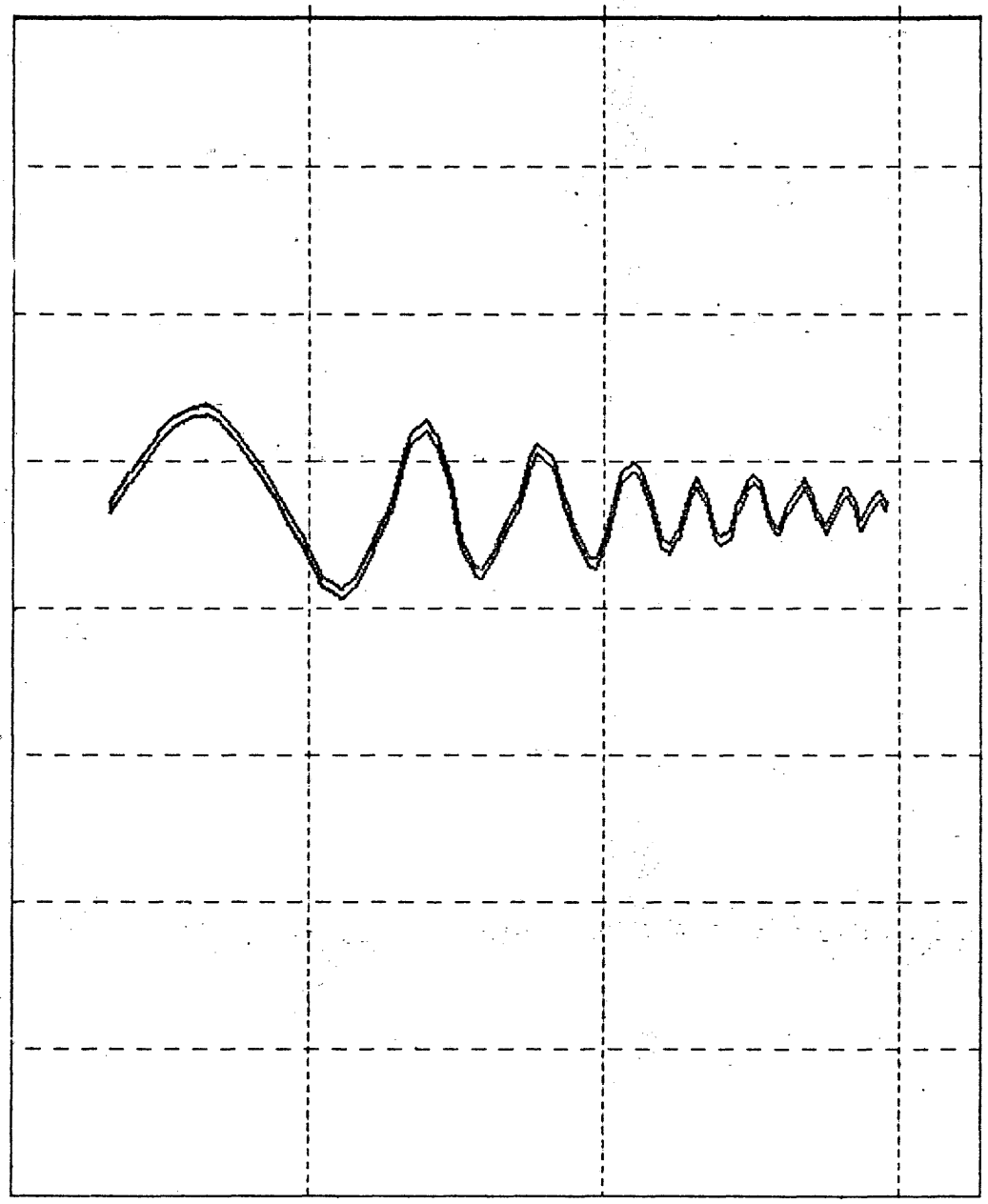

FIGURE 25.

Model of interbed in salt to test the effect of folding of thinbeds on the seismic section.

1 Km.
H=V

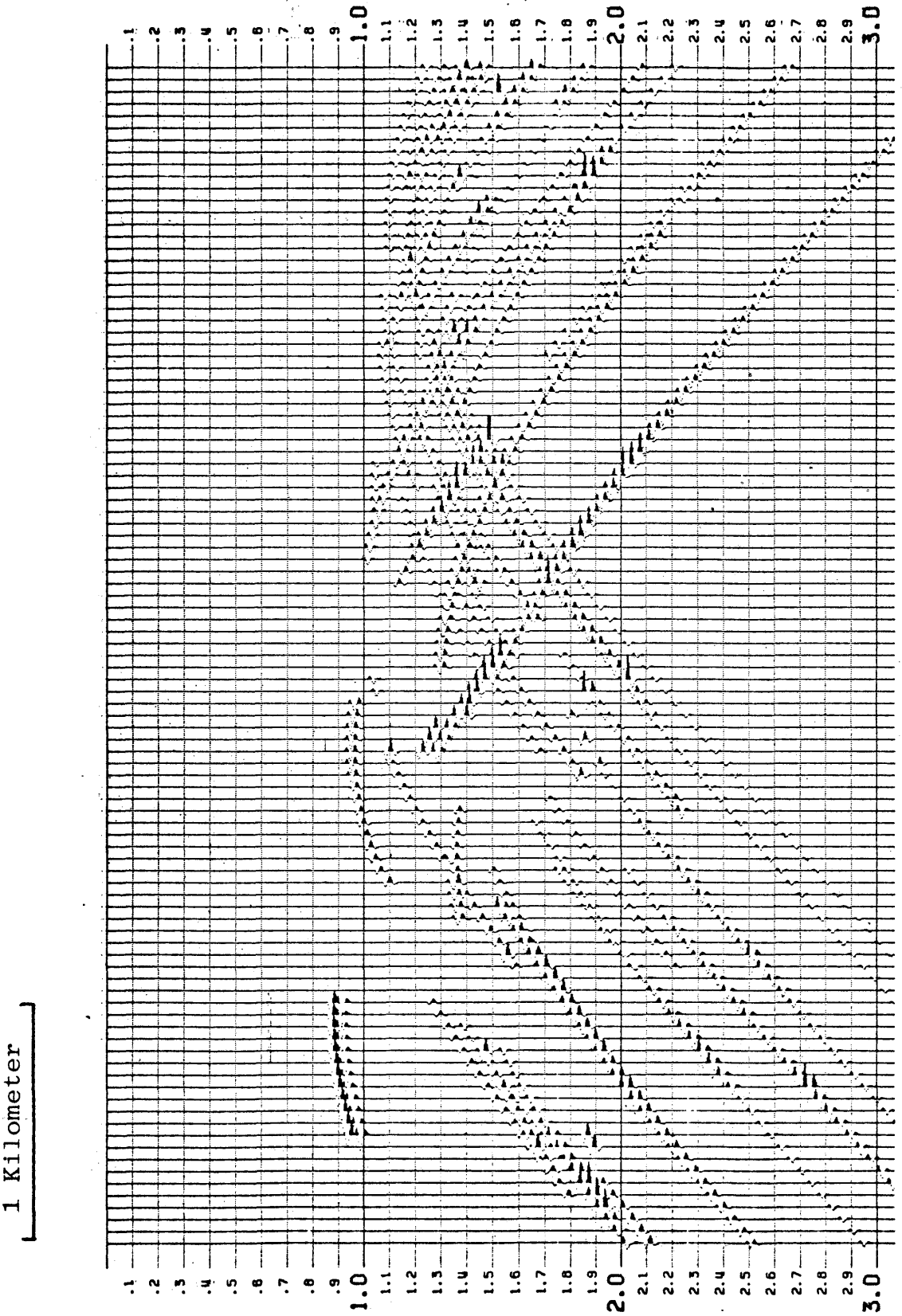

FIGURE 26.
Buried Foci from Folded Interbeds.

and degree of closure of the folds as well as the depth of the interbed to obtain foci. However, if the shape of the interbed distortion conforms to the assumptions of Hite and Lohman (1973), this technique for mapping the interbeds is feasible. Fig. 27 shows a typical salt ridge subsurface model derived from a composite of the three seismic profiles, the borehole information, and assumptions on the nature of the shallow faulting. Normally incident ray tracing was performed in order to formulate a synthetic seismic section and to determine the extent of the structurally-induced distortion of the seismic response. The normally incident rays are those which may be recorded by placing the source and receiver at the same surface location. In this manner, the transmitted and reflected seismic energy follow the same travel paths in the subsurface. Furthermore, normal moveout is eliminated as is mode conversion of the seismic waves permitting an ideal representation of the seismic response of a complex subsurface.

Snell's Law:

$$V_1 \sin \theta_2 = V_2 \sin \theta_1 \qquad \text{(Sheriff, 1973)},$$

where: V_n = The rock velocity in layer n.

θ_n = The angle of incidence or refraction in layer n.

is observed at all interfaces. For the models which appear in this paper, the acoustic properties (velocity and density) within a given lithology were assumed to be constant with depth. That is, the velocity vs. depth functions as well as the density vs. depth functions were piecewise con-

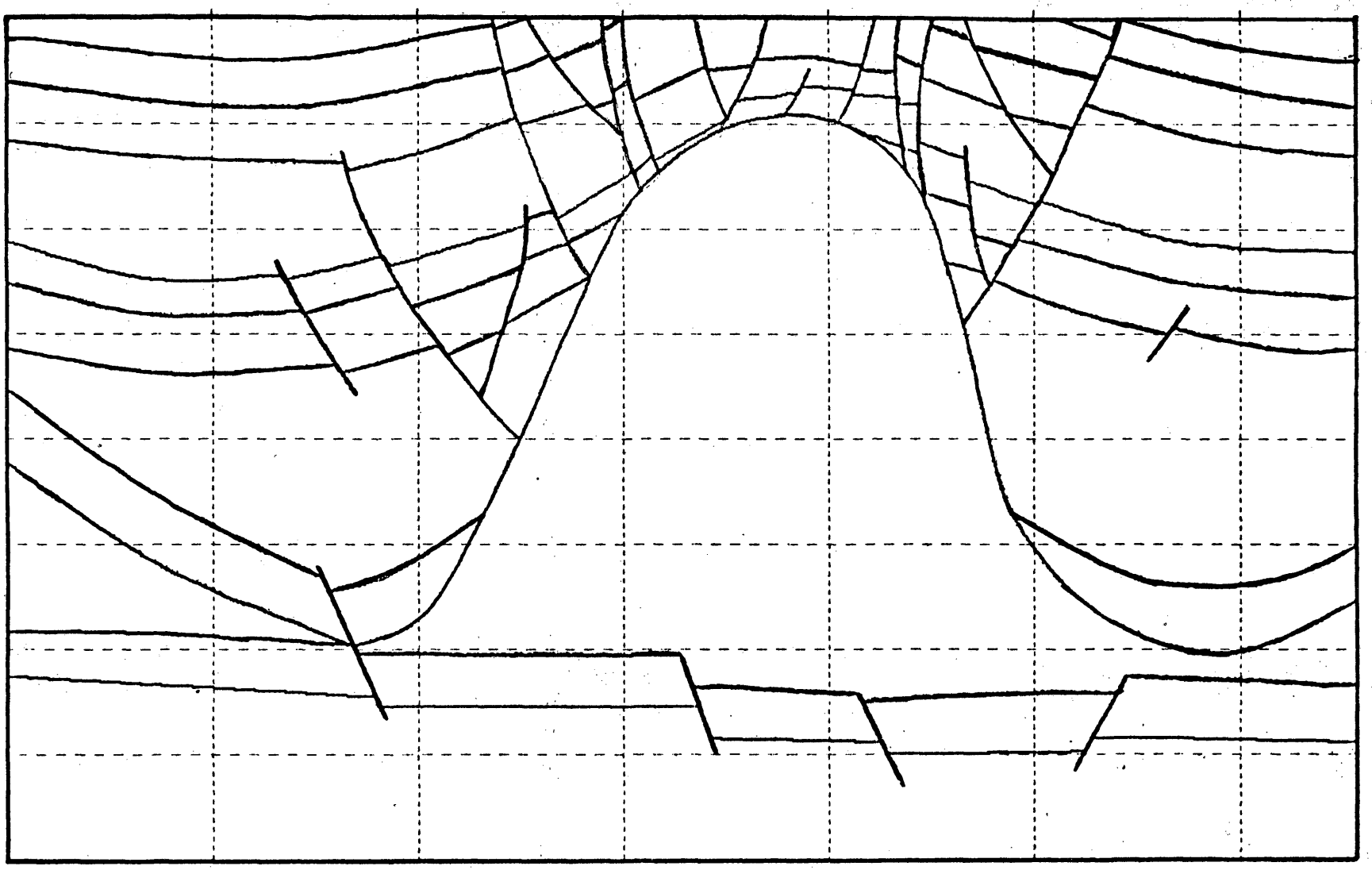

2 Kilometers
H=V

FIGURE 27.
SALT RIDGE MODEL

tinuous with jump discontinuities at defined lithologic boundaries (Fig. 28) even though this is not generally the case in the real world. Interval velocity assumptions were derived from the acoustic log data and rock densities were constructed from empirical studies by Gardner and others (1974) (Fig. 29), and Christensen (1966) with adjustments made for age, depth of burial, and lithology. Fig. 30 depicts the normally incident rays generated for the subsurface model of Fig. 27. It can be seen that the refraction of the rays at each interface has the effect of scattering the reflected energy from a small portion of the subsurface over a large portion of the time section. This emphasizes that reflections displayed vertically on a time section represent vectors in space and not necessarily a geologic depth section. The subsurface geometry and shallow faulting and the resultant acoustic boundaries tend to produce the "dead zone" in the area directly under the salt on the seismic section (Fig. 31).

The hypothetical cross-section proposed by Hite and Lohman (1973) of the Paradox Valley anticline was modeled using three assymetrically folded thin beds within the salt (Fig. 32). Second order folding was superimposed on these thin beds as was laterally varying velocity and density. Structural complexity of the interbeds was increased toward the anticlinal core in the manner of Kupfer (1965). The resultant synthetic seismic section is shown in Fig. 33. Fig. 34 shows a synthetic produced from the reflections from the interbeds only. Energy dispersion and diffractions are evident throughout the section. Many of the

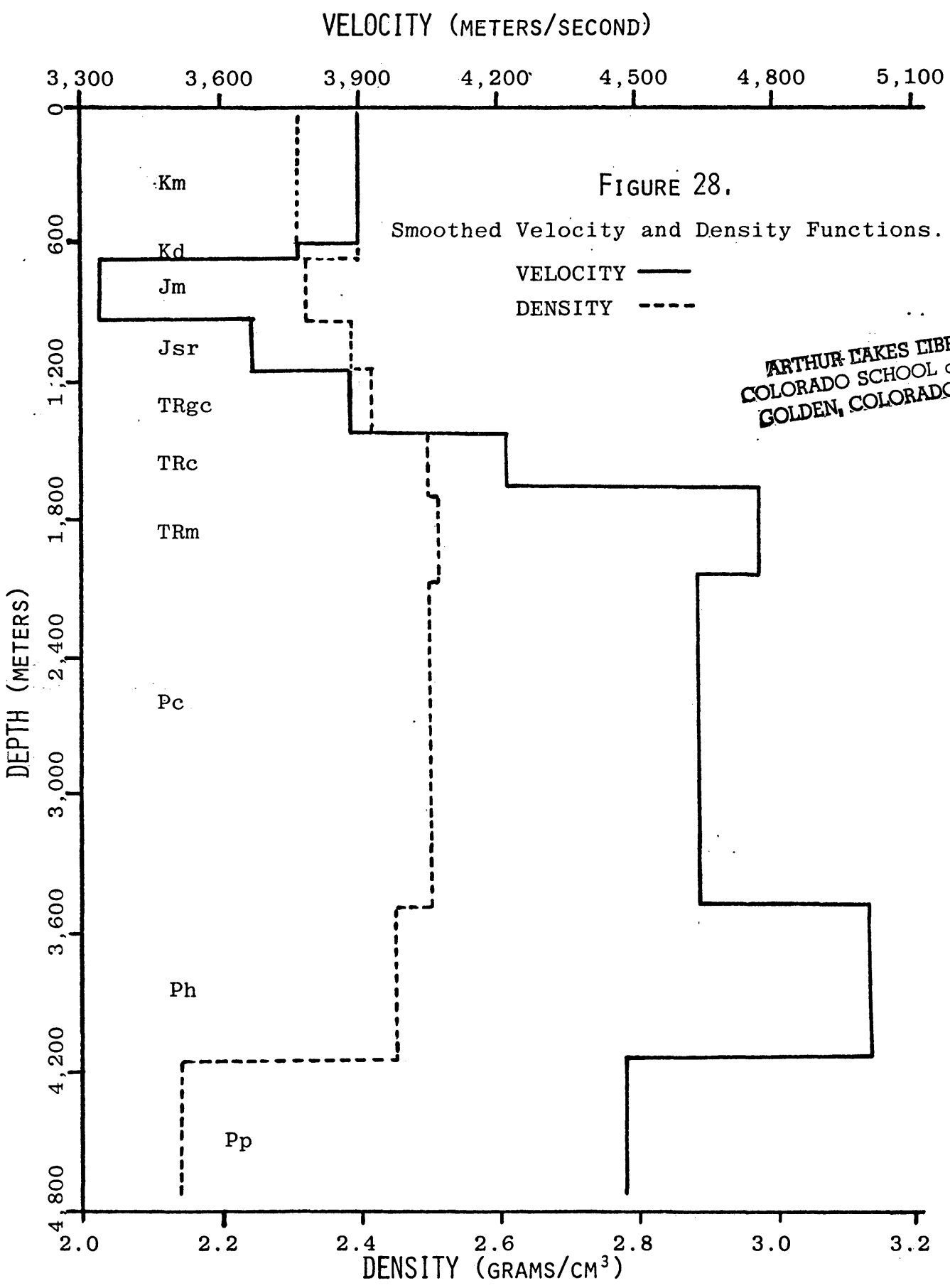

FIGURE 28.

Smoothed Velocity and Density Functions.

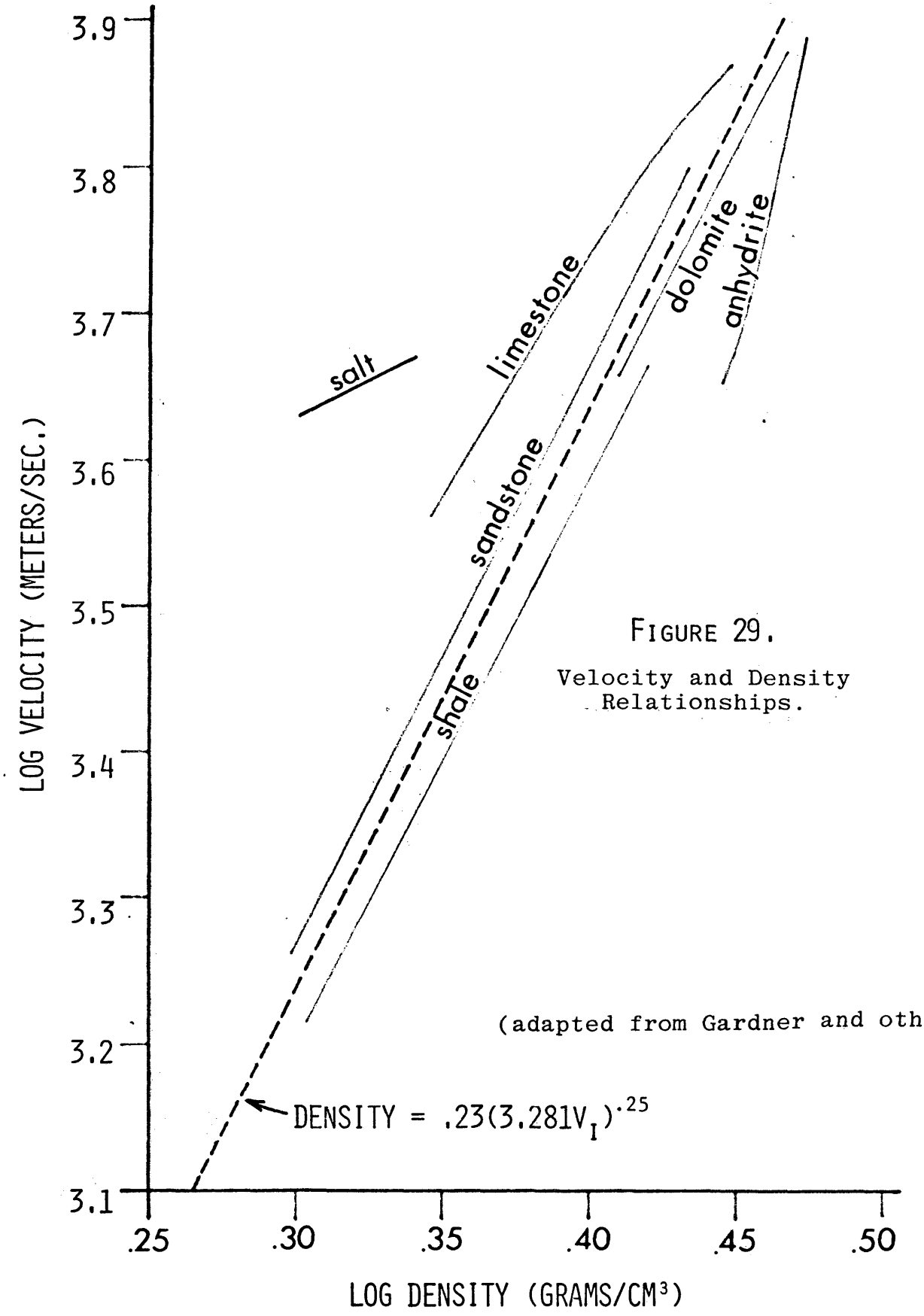

FIGURE 29.

Velocity and Density Relationships.

(adapted from Gardner and others, 1974)

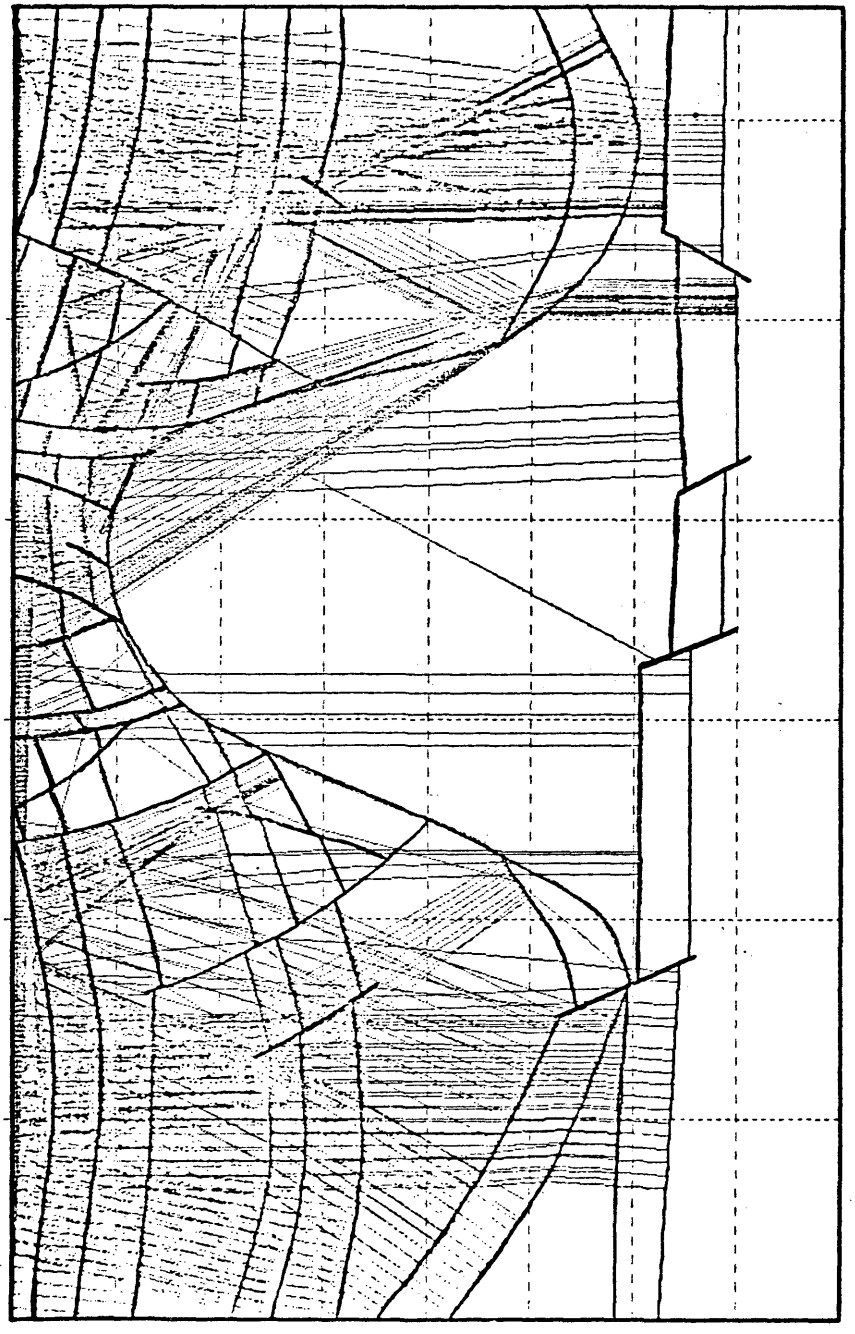

FIGURE 30.

NORMALLY INCIDENT RAYS

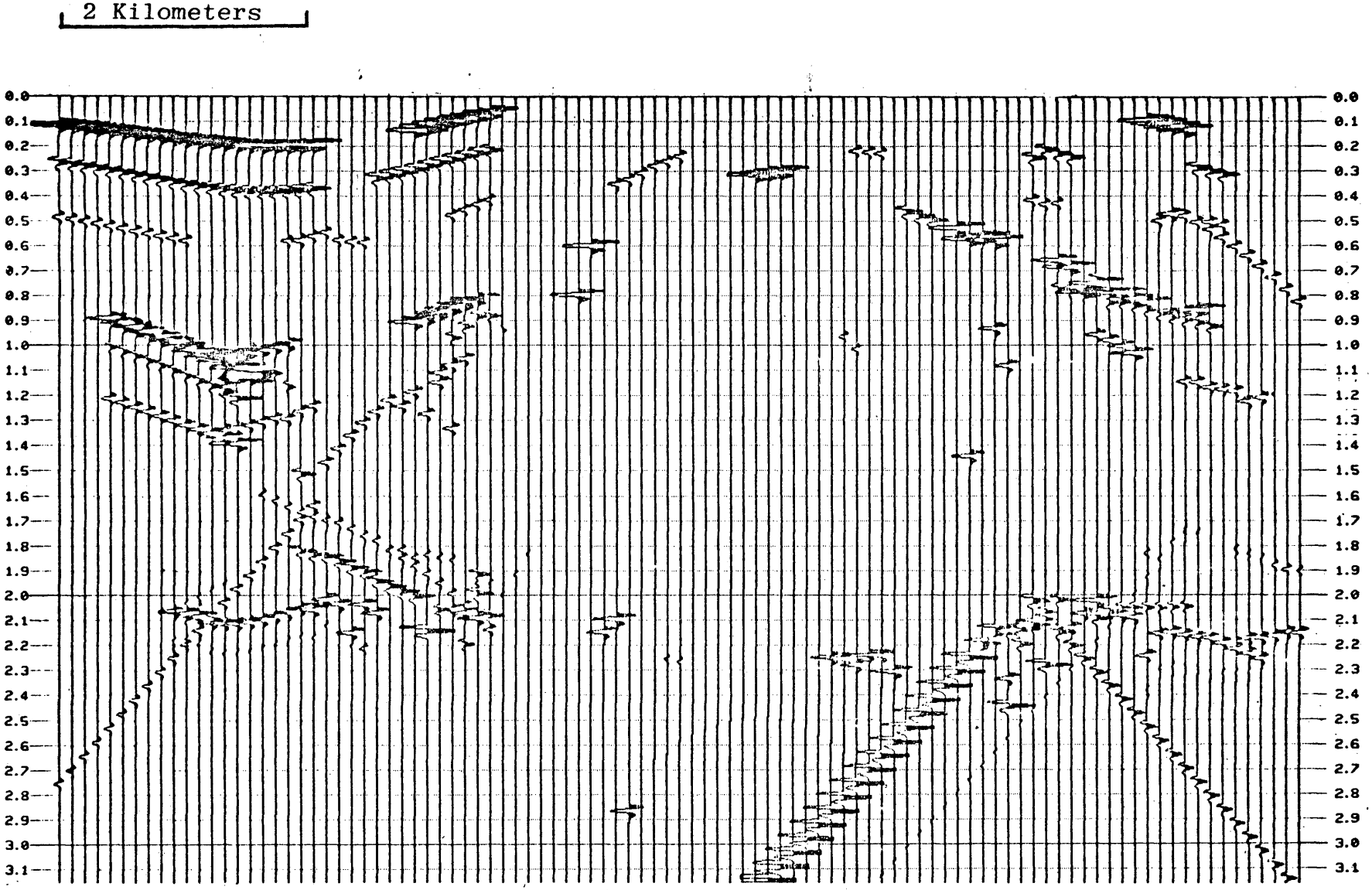

FIGURE 31.

Salt Ridge Synthetic.

This model, like all others in this paper, maintains true relative amplitudes within the dynamic range of 16 bits.

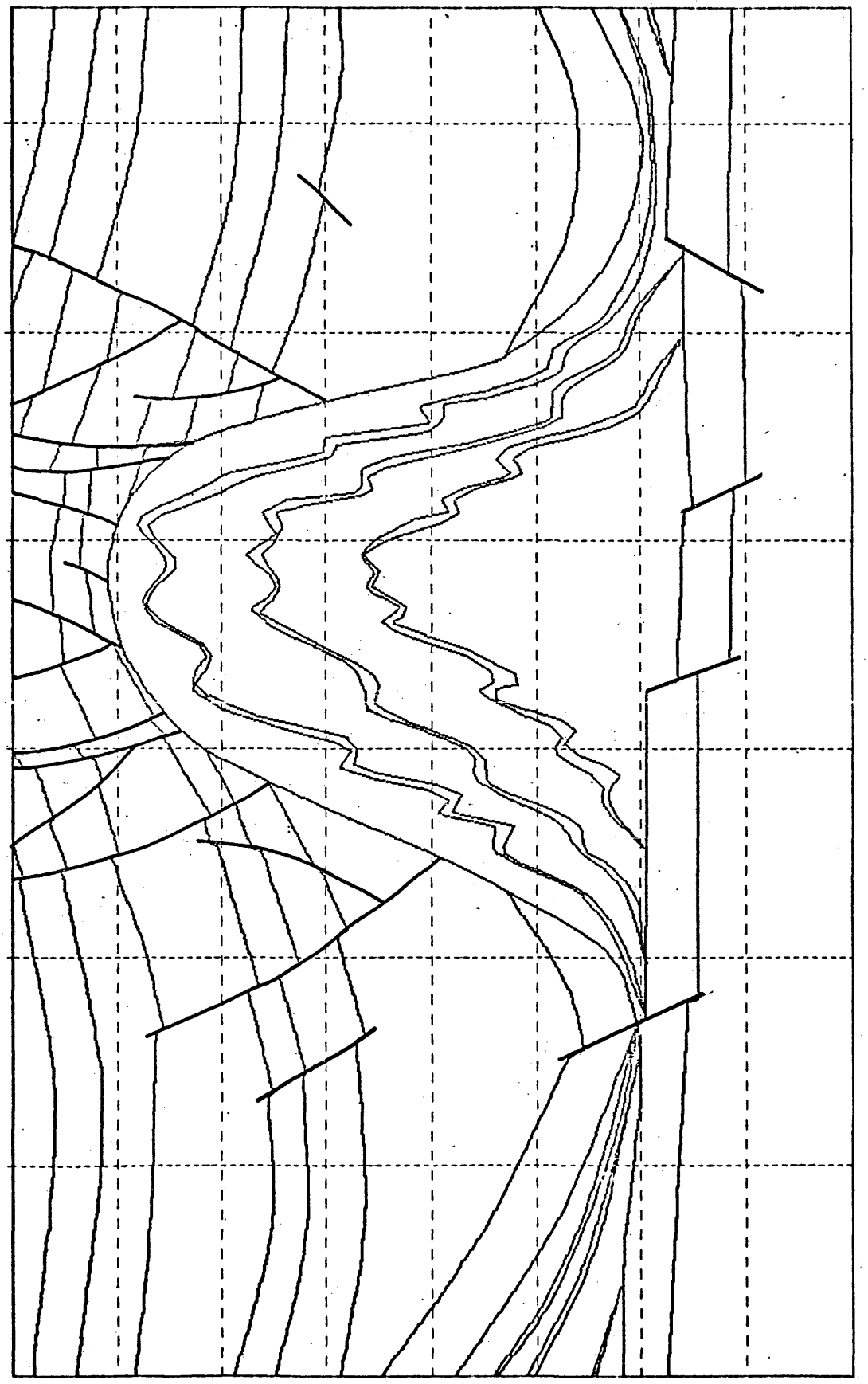

FIGURE 32.

Salt Ridge with Interbeds Modeled after Hite and Lohman, 1973.

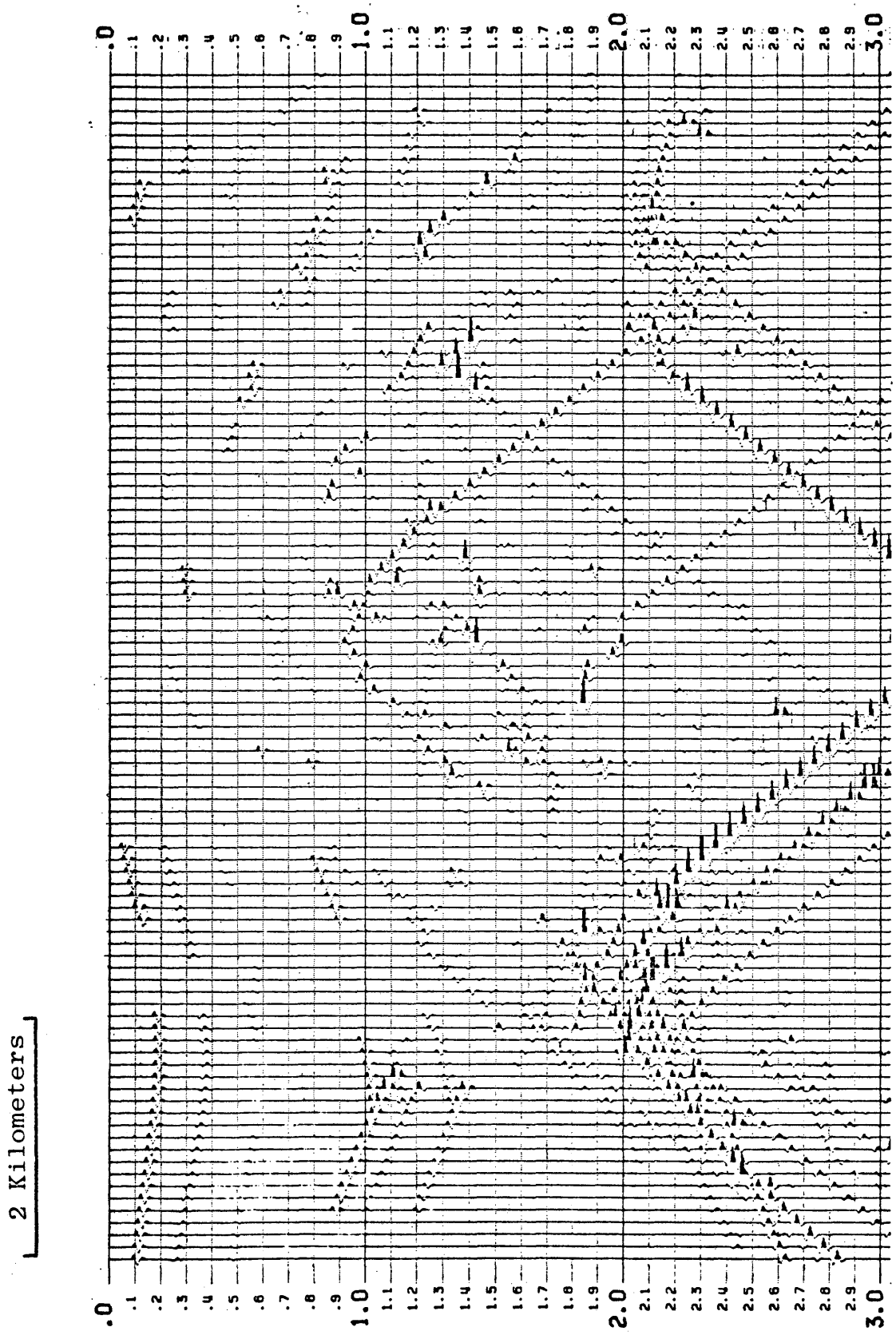

FIGURE 33.

Salt interbeds synthetic after Hite and Lohman, 1973.

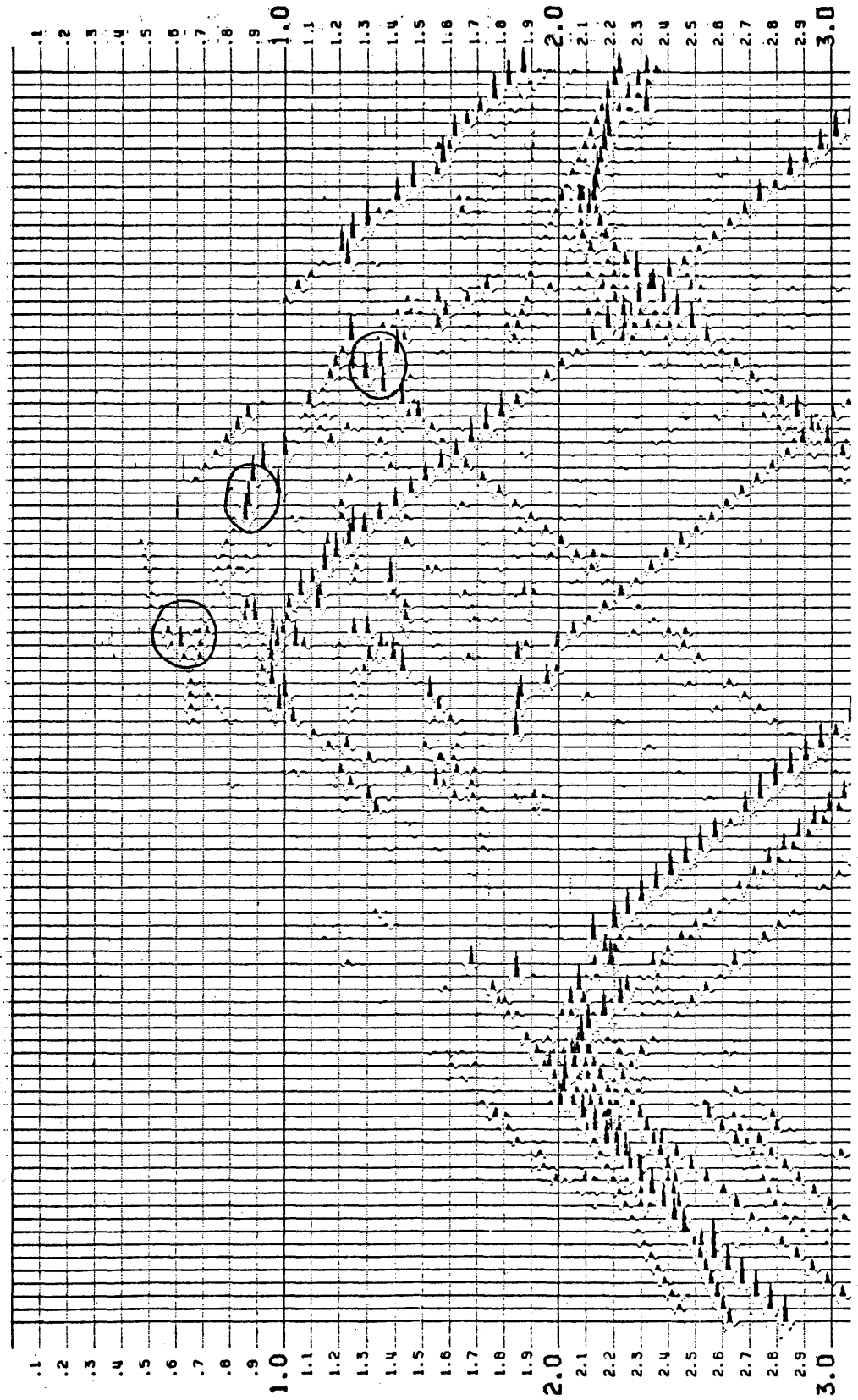

FIGURE 34

SALT RIDGE MODEL - INTERBED REFLECTIONS ONLY.

Circled areas indicate similarities to observed seismic events on real data (see Fig. 6).

folds were tighter than the 100 meter trace interval making identification of the buried foci impossible. Diffraction migration of this data would aid the detection of the interbeds, but would require a high degree of precision in the determination of the migration velocities. The diffraction migration of the synthetic data would collapse the diffractions from the tight interbed folding and yield an intra-salt en echelon pattern similar to that observed on the real seismic data (compare circled areas on Fig. 34 and Fig. 6).

The second salt ridge model has an identical flank subsurface, but less severe folding of the interbeds near the anticlinal axis (Fig. 35). This type of folding would be expected if the primary stress axis was vertical rather than horizontal. The synthetic section, again showing only reflected energy from the interbeds, is presented in Fig. 36. While the seismic response shows a proportional reduction in complexity, diffracted energy still dominates the seismic section. If, however, the shallower interbeds are of this less complex form, mapping may be possible using conventional or nearly-conventional seismic reflection techniques.

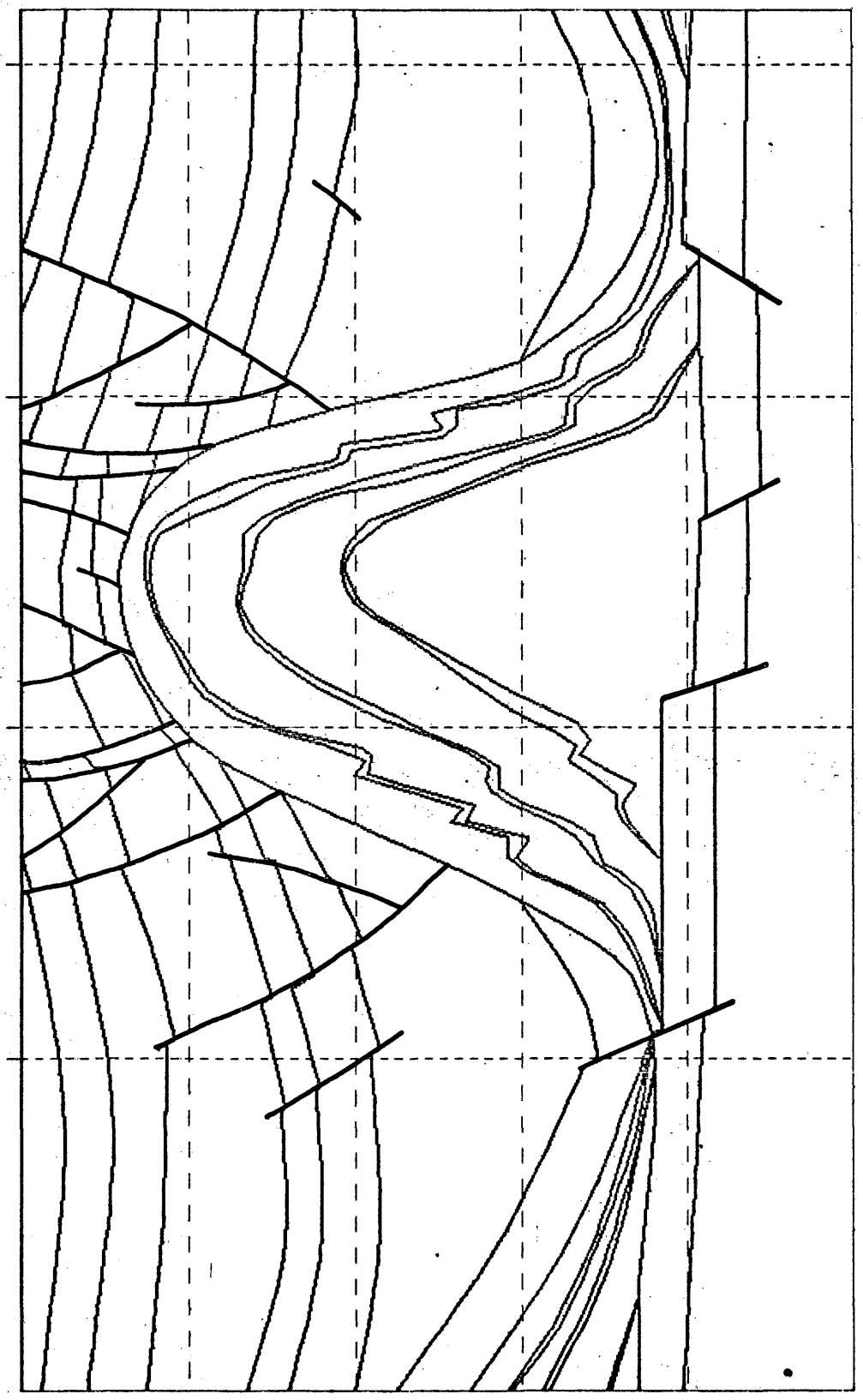

2 Kilometers
H=V

FIGURE 35.

Salt Ridge Model with less complexly folded interbeds. This type of distortion normally results from vertical stress as the principal structural mechanism.

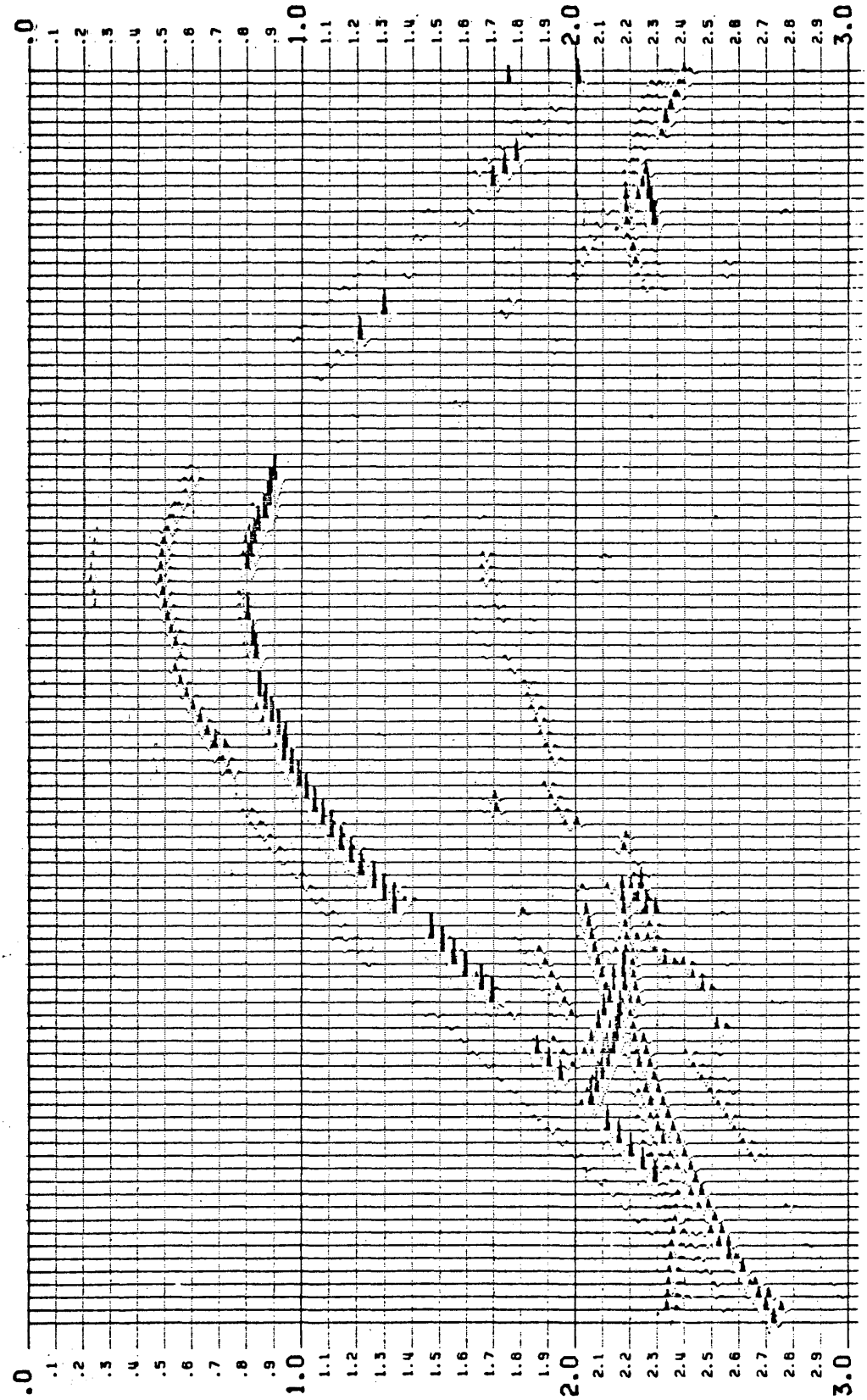

FIGURE 36.

LESS COMPLEX MODEL - INTERBED REFLECTIONS ONLY.

RECOMMENDATIONS

Mapping of shallow, structurally-complex reflectors in an area such as the Salt Valley anticline requires a custom designed integrated geophysical program incorporating state-of-the-art techniques such as: vertical seismic profiling; shallow reflection and refraction surveys, possibly using a source with an extractable signature; and a detailed borehole survey. Potential field methods, such as gravity and magnetic anomaly mapping, may have limited usefulness due to the suspected broad areal extent of the interbeds and the complexity of the near surface rocks. Moreover, recent advances in seismic data processing may yield a more quantitative analysis of the subsurface and provide greatly expanded resolution of subtle acoustic differences in the geologic profile.

Vertical Seismic Profiling

Until recently, very little attention has been accorded in the literature to the use of vertical seismic arrays in the detailing of shallow acoustic boundaries. Studies by Gal'perin (1974) and Wuenschel (1976) and others have only recently begun to exploit the advantages of vertical seismic profiling as an exploration tool. Some of the advantages of VSP are:

1. Improved signal-to-noise ratio. Placing both the source and the receiver arrays in a borehole below the inhomogeneous near surface reduces wave scattering encountered with surface or near surface

arrays.

2. Broader bandwidth is obtainable due to better rock coupling of both the source and the receiver. Expansion of the frequency bandwidth results in pulse compression in the time domain (Stone, 1973) allowing the separation of closely spaced or thin reflectors on a seismic time section.

3. Directional sensitivity of the three-component geophones normally used in vertical seismic profiling would make possible three-dimensional analysis of the seismic response yielding dip information, in addition they would allow the determination of reflector characteristics from amplitudes and modes of wave propagation.

4. In thin beds, with high density-velocity product contrasts (on the order of 2 to 1), channel-guided waves have been shown to be effective in determining interbed continuity (Guu, 1975). Vertical seismic profiling would allow the extrapolation of interbeds from areas where their identity is known into the Salt Valley anticline and be invaluable in defining the various interbed cycles.

Surface Seismic Methods

Since the principal zone of interest for a nuclear waste emplacement site is shallow (less than 1,200 meters), a short offset, small geophone-interval, surface configuration is needed. When the angle of incidence of the seismic wave with the reflectors is more nearly normal, the effects of refraction and mode conversion of the seismic energy are

minimized. In addition, if the reflected seismic wave is approximately planer when it reaches the detectors, separation of the reflected energy from horizontally-travelling noise (along the surface of the ground) is simplied. Therefore, a spread length on the order of 1,000 meters or less would insure that the angle of incidence, for a flat reflector, would be less than 30° for all traces at the depth of interest. The short offset would further insure that the Rayleigh and Love waves generated by the source would not interfere with shallow reflected energy. The depths of interest on a shallow seismic profile would be represented in less than .600 seconds of two-way-time on the seismic section. The small geophone spacing would have two advantages:

1. There would be a closer grid spacing on the subsurface reflection profile equal to one half on the geophone spacing. This would allow detection of smaller anomalies on the reflectors.

2. More geophones would allow higher common-depth-point multiplicity and provide better noise cancellation.

Exact field recording configurations should be established after sufficient noise analysis to determine the optimum source and geophone configuration for best noise cancellation.

Reflection and refraction seismic data should be capable of providing very high resolution of the subsurface. For an interbed 15 meters thick with an interval velocity of 3,000 meters/second, a seismic pulse only .01 seconds wide would be needed. Therefore, for this reflector, frequencies of at least 100 hertz must be resolved without aliasing.

The Nyquist, or aliasing frequency for digitized data is defined as:

$$F_n = \frac{1}{2\Delta t}$$

where: Δt = The digitizing interval (sample rate) measured in seconds. Frequencies above Nyquist are indistinguishable from lower frequencies on a digitized seismic trace. Since distortion (although not aliasing) usually occurs above half Nyquist, a recording system should be capable of digitizing the data on a .002 second or smaller sampling interval (ie. F_n = 250 hertz). For thinner interbeds or higher velocities, a smaller sampling rate would be required. A .00025 second ($\frac{1}{4}$ ms.) sampling interval would be much better for detection of very thin, high velocity interbeds. Burial of the geophones would ensure that ground coupling was optimized and that the higher frequency seismic data would be detectable.

The source signature can be controlled and recorded with the data on some field systems. This signature may then be removed from the data via a cross-correlation method. Several recent advances in field system design have made possible a controlled source signature in addition to the extremely small sampling rate. In this manner, a non-impulsive source can introduce a signal into the earth with frequency and time domain characteristics which best match the natural frequencies associated with the lithologies under investigation.

Refraction surveys have long been established as a method for mapping in detail, the irregular near surface layer. Long source-receiver offsets are used to record refracted energy which travels along the inter-

face between the low velocity, uncompacted, near surface layer and the deeper, more competent, higher velocity layer. Refraction shooting would yield an accurate estimate of shallow velocities and interval thicknesses needed to establish control on velocity and static corrections to datum.

Borehole Geophysics

All of the seismic surface and vertical seismic profiling could be effectively tied to the geology using carefully positioned wells drilled to the depth of interest. These holes should be planned for use in conjunction with the vertical seismic profiling. Logging technology has advanced to the state where detailed mapping of very thin beds to a high degree of precision is now possible. Some of the log types available which have direct applications to the stratigraphic and structural evaluation of the Salt Valley anticline are:

1. Acoustic log - As already demonstrated in this report, this tool measures the interval transit time (inverse rock velocity) and can be used to tie seismic reflection data to geology and to generate synthetic seismograms.

2. Dip log - This log quantitatively measures the orientation of bedding planes at their point of intersection with the well. Such a log would be useful in analyzing the structural complexity of the interbeds and in interpolating interbeds between wells.

3. Gamma Ray/Neutron log - These logs measure the level of radioactivity in the rock. This would be especially useful in identifying very thin interbeds containing trace amounts of potash or clay minerals.

Potassium 40 is a radioactive isotope commonly found in the interbeds and provides a high radioactive contrast with the salt.

CONCLUSIONS

From this study, the following results and conclusions are made:

a.) Analysis of approximately 50 kilometers of conventional reflection seismic data using surface arrays and both impulsive and controlled sources indicates that the potential exists for mapping of shallow, high acoustic contrast isolated thin beds in a homogeneous salt.

b.) Computer ray-trace modeling has aided in identification of frequency and spatial resolution limitations present in most petroleum seismic data. For more detailed mapping of very thin (5 - 70 meters), intensely-folded interbeds at depths of less than 750 meters, frequencies on the order of 500 to 1000 hertz and surface array lengths of less than 350 meters are recommended. Furthermore, consideration should be given to burial of both the source and receiver arrays in order to attenuate surface related noise.

c.) Correlation of the reflection seismic data with available well data and surface geology in the area of the salt-cored anticlines in the Paradox basin of southeastern Utah indicates a complex structurally initiated, basement fault controlled piercement salt diapir whose upward momentum was influenced by contemporaneous deposition of Permian continental clastics in the adjacent synclines formed by removal of the salt. Collapse faulting due to solution near the crests of these diapirs is responsible for distortion of the seismic response.

c.) Evidence exists that thin interbeds of anhydrite, dolomite and black shale are mappable either as anomalous amplitudes due to buried

focusing or as short, discontinuous segments. Computer modeling of folded thin beds in salt confirms both of these as possible causes for the intra-salt seismic response observed on the seismic reflection profiles.

d.) The seismic signatures from the interbeds can be predicted from computer simulation of the subsurface geometry and acoustic properties. For impulsive source data, a minimum phase wavelet is a good approximation to the expected signature. However, as the thickness of the interbed approaches the period of the assumed wavelet, interference between the reflections from the two adjacent acoustic boundaries (interbed top and bottom) distorts the signature and a symmetric response results.

e.) Refinements of existing seismic reflection methods and integration with other geophysical techniques should allow more direct identification of the interbeds in salt. These methods should include:

1.) Vertical seismic profiling.

2.) A shallow, short-offset, high-multiplicity, high-frequency seismic reflection survey.

3.) A detailed borehole survey.

f.) Results of this study may provide guidelines for an informed approach to other geophysical problems requiring detailed mapping of thin, high acoustic impedance contrast layers in a homogeneous medium.

REFERENCES

Anstey, N. A., 1966, Correlation display pinpoints seismic multiples: Seismograph Service Limited, internal publication, 12p.

Balk, Robert, 1949, Structure of Grand Saline salt dome, Van Zandt County, Texas: Amer. Assoc. Petroleum Geologists Bull., V. 33, no. 11, p. 1791-1829.

Barton, D. C., 1933, Mechanics of formation of salt domes with special reference to Gulf Coast salt domes of Texas and Louisiana: Amer. Assoc. Petroleum Geologists Bull., V. 17, p. 1025-1083.

Biot. M. A., 1964, Theory of internal buckling of a confined multilayered structure: Geol. Soc. America Bull., V. 75, p. 563-568.

Cater, Fred W., 1970, Geology of the Salt Anticline Region in southwestern Colorado: U. S. Geol. Survey Prof. Paper 637, 80p.

Christensen, Dean M., 1966, The determination of insitu elastic properties of rock salt with a 3-dimensional velocity log, in Second Symposium on Salt: Northern Ohio Geol. Soc., V. 2, p. 104-115.

Claerbout, Jon F., 1976, Fundamentals of geophysical data processing: McGraw-Hill Book Co., Inc., 274p.

Elston, D. P., and Landis, E. R., 1960, Pre-Cutler unconformities and early growth of the Paradox Valley and Gypsum Valley salt anticlines, Colorado, in Short papers in the geological sciences: U. S. Geol. Survey Prof. Paper 400-B, p. B261-B265.

Evans, Robert, and Linn, Kurt O., 1970, Fold relationships within evaporites of the Cane Creek anticline, Utah, in Third Symposium on Salt: Northern Ohio Geol. Soc., V. 1, p. 286-297.

Gal'perin, E. I., 1974, Vertical seismic profiling: SEG Special publication, no. 12, 270p.

Gardner, G. H. F., Gardner, L. W., and Gregory, A. R., 1974, Formation velocity and density - the diagnostic basics for stratigraphic traps: Geophysics, V. 39, no. 6, p. 770-780.

Geyer, Robert L., 1970, The Vibroseis system of seismic mapping: Journal of the Canadian Society of Exploration Geophysicists, V. 6, no. 1, p. 39-57.

Gussow, William C., 1960 Salt diapirism: importance of temperature and energy source of emplacement, in Diapirism and Diapirs - a Symposium; memoirs: Amer. Assoc. of Petroleum Geologists, 1968, p. 16-52.

Guu, Jeng-Yih, 1975, Studies of seismic guided waves: the continuity of coal seams: Colorado School of Mines Thesis, 85 p.

Hite, R. J., 1960, Stratigraphy of the saline facies of the Paradox Member of the Hermosa Formation of southeastern Utah and southwestern Colorado, in Geology of the Paradox basin fold and fault belt: Four Corners Geol. Soc. Guidebook 3rd Field Conf., 1960, p. 86-89.

_____ 1961, Potash-bearing evaporite cycles in the salt anticlines of the Paradox basin, Colorado and Utah, in Short papers in the geologic and hydrologic sciences: U. S. Geol. Survey Prof. Paper 424-D, p. D135-D138.

Hite, R. J., and Lohman, S. W., 1973, Geologic appraisal of Paradox basin salt deposits for waste emplacement: U. S. Geol. Survey Open-file Report, 75p.

Kupfer, Donald H., 1965, Relationship of internal to external structure of salt domes, in Diapirism and Diapirs - a Symposium; memoirs: Amer. Assoc. of Petroleum Geologists, 1968, p. 172-181.

_____ 1974, Shear zones in Gulf Coast salt delineate spines of movement, in Transactions - Gulf Coast Association of Geological Societies, V. 24, p. 197-208.

LeFond, Stanley J., 1969, Handbook of world salt resources: Plenum Press, p. 21.

Levinson, N., 1947, The Wiener RMS (root mean square) error criterion in filter design and prediction: Journal of Mathematics and Physics, V. 25, p. 261-278.

Lindseth, Roy O., 1967, The nature of digital seismic processing: Journal of the Canadian Society of Exploration Geophysicists, V. 3, no. 1, p. 31-111.

Nettleton, L. L., 1934, Fluid mechanics of salt domes: Amer. Assoc. Petroleum Geologists Bull., V. 18, no. 9, p. 1175-1204.

Peterson, James A., and Ohlen, Henry R., 1963, Pennsylvanian shelf carbonates, Paradox basin, in Shelf Carbonates of the Paradox Basin: Four Corners Geol. Soc. - A Symposium 4th Field Conf., p. 65-79.

Ricker, N., 1953, The form and laws of propagation of seismic wavelets: Geophysics, V. 18, no. 1, p. 10-40.

Rieber, Frank, 1937, Complex reflection patterns and their geologic sources: Geophysics, V. 2, no. 2, p. 132-160.

Sheriff, R. E., 1973, Encyclopedic dictionary of exploration geophysics: Society of Exploration Geophysicists, 266p.

Slotnick, M. M., 1936, On seismic computations with applications, I: Geophysics, V. 1, no. 1, p. 9-22.

Stone, Dale G., 1973, Pulse compression for seismic data: Contribution to European Assoc. of Exploration Geophysicists, 35th annual meeting, June 1973, (preprint).

Tanner, W. F., and Williams, G. K., 1965, Model diapirs, plasticity and tension, in Diapirism and Diapirs - a Symposium; memoirs: Amer. Assoc. of Petroleum Geologists, 1968, p. 10-15.

Treitel, Sven, Shanks, John L., and Frasier, Clint W., 1967, Some aspects of fan filtering: Geophysics, V. 32, no. 5., p. 789-800.

Williams, Emyr, 1961, The deformation of confined, incompetent layers in folding: Geol. Magazine, V. 98, no. 4, p. 317-323.

Wuenschel, Paul, C., 1976, The vertical array in reflection seismology - some experimental studies: Geophysics, V. 41, no. 2, p. 219-232.